Microbiome

RESEARCH

Open Access

Combating wheat yellow mosaic virus through microbial interactions and hormone pathway modulations

Fangyan Wang[1], Haoqing Zhang[1*], Hongwei Liu[2], Chuanfa Wu[1], Yi Wan[1], Lifei Zhu[1], Jian Yang[1], Peng Cai[3], Jianping Chen[1] and Tida Ge[1*]

Abstract

Background The rhizosphere microbiome is critical for promoting plant growth and mitigating soil-borne pathogens. However, its role in fighting soil-borne virus-induced diseases, such as wheat yellow mosaic virus (WYMV) transmitted by *Polymyxa graminis* zoospores, remains largely underexplored. In this study, we hypothesized that during viral infections, plant microbiomes engage in critical interactions with plants, with key microbes playing vital roles in maintaining plant health. Our research aimed to identify microbial taxa that not only suppress the disease but also boost wheat yield by using a blend of techniques, including field surveys, yield assessments, high-throughput sequencing of plant and soil microbiomes, microbial isolation, hydroponic experiments, and transcriptome sequencing.

Results We found that, compared with roots and leaves, the rhizosphere microbiome showed a better performance in predicting wheat yield and the prevalence of *P. graminis* and WYMV across the three WYMV-impacted regions in China. Using machine learning, we found that healthy rhizospheres were marked with potentially beneficial microorganisms, such as *Sphingomonas* and *Allorhizobium-Neorhizobium-Pararhizobium-Rhizobium*, whereas diseased rhizospheres were associated with a higher prevalence of potential pathogens, such as *Bipolaris* and *Fusicolla*. Structural equation modeling showed that these biomarkers both directly and indirectly impacted wheat yield by modulating the rhizosphere microbiome and *P. graminis* abundance. Upon re-introduction of two key healthy rhizosphere biomarkers, *Sphingomonas azotifigens* and *Rhizobium deserti*, into the rhizosphere, wheat growth and health were enhanced. This was attributed to the up-regulation of auxin and cytokinin signaling pathways and the regulation of jasmonic acid and salicylic acid pathways during infections.

Conclusions Overall, our study revealed the critical role of the rhizosphere microbiome in combating soil-borne viral diseases, with specific rhizosphere microbes playing key roles in this process.

Keywords *Triticum aestivum* L, Soil-borne viral disease, *Polymyxa graminis*, Plant-associated microbiome, Rhizosphere, Jasmonic acid, Salicylic acid

*Correspondence:
Haoqing Zhang
zhanghaoqing@nbu.edu.cn
Tida Ge
getida@nbu.edu.cn
Full list of author information is available at the end of the article

Background

Outbreaks of various soil-borne diseases severely affect plant health, leading to productivity losses of up to 30% in a wide range of cash crops, vegetables, and fruits [1, 2]. Accumulating evidence suggests that plant-associated microbiomes are crucial for maintaining crop health through mechanisms such as pathogen combat, nutrient acquisition, and interactions with the plant immune system, which ultimately affect crop growth and productivity [3–6]. Following infection, plants can stimulate and support beneficial microorganisms to combat soil-borne pathogens. They can alter the microbial diversity, community composition and functions, transforming the microbiome from a disease-conductive to a disease-suppressive state [7–9]. These findings revealed a microbial layer of plant defense that is instrumental for developing microbiome-based approaches to manage diseases in the field. Hence, understanding and identifying key microbial taxa that regulate host defense and health are important for harnessing them to address plant diseases [10]. However, despite the importance of plant microbiomes in fighting soil-borne bacterial, fungal, and protozoan pathogens [11], how plant microbiomes respond and affect RNA virus-caused soil-borne diseases remain unclear. Whether key microbes assist plants in combating virus infections have been much less explored. Such knowledge gaps restrict the capacity to develop sustainable approaches for managing soil-borne virus-induced plant diseases.

Wheat yellow mosaic disease is a widespread soil-borne viral disease mainly caused by the wheat yellow mosaic virus (WYMV). This virus is transmitted by zoospores of the plasmodiophoraceous microorganism *Polymyxa graminis* [12] and has spread across a large scale worldwide in recent years. Wheat yellow mosaic causes significant damage to wheat yields, typically reducing them by 10–30% or up to 50–70% in serious cases [13, 14]. To control and prevent wheat yellow mosaic disease, significant efforts have been made to understand the pathogenesis of WYMV and to breed or genetically engineer cultivars with enhanced resistance to WYMV by introducing resistance genes [15]. Despite the fact that quantitative trait loci associated with disease resistance have been found [16], breeding or engineering cultivars with a large number of genes remains challenging [17]. Increasing plant WYMV resistance by manipulating plant or soil microbiomes has been touted as an alternative approach, which can potentially prevent the disease from the "source." Our previous studies found that wheat rhizosphere microbial communities and their assembly processes are involved in the occurrence of wheat yellow mosaic disease [18, 19]. However, whether there are key microbial taxa that directly or indirectly inhibit the virus and *P. graminis*, thereby maintaining wheat health and yield, is yet to be investigated.

Recent studies have viewed the interactions between pathogens, plants, the microbiome, and their surrounding environments as a new paradigm for understanding plant disease dynamics [20]. Augmenting this perspective, the model of viral infection in wheat will shed light on how viruses and their associated vectors fit into the disease paradigm. Notably, the WYMV vector, *P. graminis*, is soil-borne. The rhizosphere will be the primary site where *P. graminis* establish parasitic relationships with plants. Thus, *P. graminis* may directly interact with the rhizosphere microbiome via niche competition and collaboration. The native members in the resident rhizosphere microbiota which form partnerships and competitive relationships with *P. graminis* will collectively impact virus-induced diseases in wheat plants. Moreover, the reassembled rhizosphere microbes regulate the plant resistance to viral diseases not only through directly interact with vectors [21–23] but also through induced systemic resistance (ISR) of host plants, which is mediated by plant immunity-associated phytohormones such as salicylic acid (SA) and jasmonic acid (JA) [24, 25]. Based on the above concepts, we hypothesized that (i) compared to other parts of the plant, the rhizosphere microbiome has a stronger response and plays a more important role in preventing wheat yellow mosaic disease and maintaining yield, (ii) diseased wheat plants are associated with a pathobiomes composed of potential pathogens in the rhizosphere that facilitates WYMV infection, and (iii) specific microbes colonizing the healthy rhizosphere minimize viral infections by inducing the ISR of the aboveground parts, thereby maintaining plant health [26, 27].

To test these hypotheses, we conducted comprehensive field surveys across three geographically distinct wheat cropping fields in Shandong, Jiangsu, and Henan, China, which were chosen because of their significant geographical separation. This approach allowed us to investigate the effects of disease infection on wheat yields in various environments. By examining these widely separated fields, we aimed to understand regional variations in the effects of WYMV and the role of rhizosphere microbiomes in different soil and climatic conditions. To explore the role of microbiomes in the interactions of wheat with the virus and its vector, we examined the differences in bacterial, fungal, and protozoan communities across different plant compartments of healthy and diseased wheat. We then identified the key microbial taxa that suppressed the disease and maintained wheat yield using a machine-learning approach. Finally, we successfully isolated these key microbes from the rhizosphere, tested their plant growth-promoting and virus-resistant

effects, and investigated the molecular mechanisms of their interactions via in vivo tests and RNA sequencing (RNA-seq) of plant tissues. Using these combined techniques, along with careful validation experiments, our findings revealed the vital role of rhizosphere microbiomes in fighting soil-borne viral diseases and highlighted the potential of specific microbes in maintaining plant health.

Methods

Sample collection

Soil and plant samples were collected from winter wheat fields at three sites located in Junan, Shandong Province (site 1: 35°11' N, 118°64' E); Yangzhou, Jiangsu Province (site 2: 32°89' N, 119°63' E) and Zhumadian, Henan Province (site 3: 33°22' N, 114°02' E) in China. These locations span from a temperate monsoon zone to a subtropical humid zone. Among them, Junan (site 1) has a temperate monsoon climate, with an annual rainfall of 840 mm and temperature of 13.4℃. Yangzhou (site 2) has a subtropical humid climate, with an annual rainfall of 1020 mm and temperature of 14.8℃. Zhumadian (site 3) has the dual characteristics of subtropical humid and temperature monsoon climates. The annual rainfall in Zhumadian is 860–980 mm and the annual temperature is 14.8℃. The soils at these sites are classified as aquic brown soil, yellow brown earth, and fluvo-aquic soil, respectively. Winter wheat has been sown annually between November and December in each field for over a decade. At each site, 750 kg ha^{-1} of compound fertilizer ($N:P_2O_5:K_2O = 14:7:9$) was added and fully mixed with the soil as a base fertilizer before wheat planting. Further details of the sampling sites including the wheat varieties used in this study are listed in Table S1.

Sampling was performed during the winter wheat seedling stage in 2021, with the exact date of sampling hinge on the growth stage of the wheat at each site (Table S1). During this period, the zoospores of the *P. graminis*, which carry the WYMV begin to attach to the surface of root cells and infect wheat roots. Before sampling, the wheat fields at each site were divided into 15 plots (20 m^2) based on their historic disease conditions. These included five healthy plots, five moderately diseased plots, and five severely diseased plots. In the perennial healthy plots, no plants showed visible disease symptoms during the outbreak of wheat yellow mosaic disease for more than 5 years. In the perennial moderately diseased plots, all plants showed yellowish leaves with clear streak mosaic during the outbreak of wheat yellow mosaic disease for more than 5 years. In the perennial severely diseased plots, all plants showed deep yellow on the whole leaves, and the mortality rate was higher than 50% during the outbreak of the wheat yellow mosaic disease for more than 5 years. These 15 plots were randomly arranged in the field, and healthy and diseased plots were adjacent to each other. Five plants were randomly selected as replicates from each plot. The rhizosphere soil, roots, and leaves were collected from each plant. Specifically, wheat plants were extracted from the soil along with their surrounding earth using a shovel. The roots of each plant were gently shaken to remove the loosely adhered soil, and the residual soil attached to the roots was collected with a sterilized brush, which was considered as the rhizosphere soil [28]. Wheat roots and leaves were separated using sterilized scissors and collected individually. Finally, the soil, root, and leaf samples collected from the same plots were combined to create composite samples, resulting in 15 rhizosphere soil, 15 root, and 15 leaf samples from each site. All samples were transferred to clean sterilized bags to an icebox and immediately transported to the laboratory.

A small part of each leaf sample (~0.3 g) was cut off with sterilized scissors, transferred to a 2-ml centrifuge tube after surface sterilization, and placed in liquid nitrogen for total RNA extraction and quantification of WYMV. The protocols used for total RNA extraction and quantification of WYMV were provided in Method S1. The remaining samples were frozen at − 80°C for endophytic DNA extraction and 16S rRNA, ITS, and 18S rRNA gene amplicon sequencing. Soil samples were separated into three fractions: one part was immediately stored at − 80°C for DNA exaction, 16S rRNA, ITS, and 18S rRNA gene amplicon sequencing, and *P. graminis* quantification; another part was air-dried to assess soil chemical properties; and the remaining fresh soil was stored at 4°C for determining the ammonium nitrogen, nitrate nitrogen, dissolved organic carbon, and dissolved organic nitrogen contents. Soil properties were analyzed using previously described protocols [19, 29]. The quantification of WYMV and *P. graminis* is described in Methods S1. At the ripening stage, we harvested all wheat plants and weighed the grain yield at the three sites to assess the impact of the disease on wheat productivity. A flowchart of the field surveys and the sampling strategy is shown in Fig. 1a.

Nucleic acid extraction, 16S rRNA, ITS, and 18S rRNA genes amplicon sequencing, and sequence processing

Before the DNA of plant materials were extracted, the plant materials were surface sterilized as follows: wheat leaves and roots were treated with 30% sodium hypochlorite, followed by repeated rinsing with 70% ethanol and sterile water. Residual fluids were removed using sterilized filter paper [6]. Then, the soil and total plant DNA were extracted from fresh soil (0.5 g) and surface-sterilized plant material (0.5 g) using a Fast DNA SPIN Kit

(MP Biomedicals, Santa Ana, CA, USA) according to the instructions provided by the manufacturer. We assess the quality and quantity of DNA using a NanoDrop spectrophotometer (NanoDrop Technologies, Wilmington, DE, USA) and 1.0% agarose gel electrophoresis, respectively. Following extraction, the DNA was stored at − 20°C for further processing.

The V4 hypervariable region of the 16S rRNA gene, the internal transcribed spacer region (ITS), and the V4 hypervariable region of 18S rRNA were amplified to assess for bacteria, fungi, and protozoa, respectively. The primers were listed in Table S2. The polymerase chain reaction (PCR) conditions employed were as follows: 95°C for 3 min, followed by 35 cycles of 95°C for 30 s, 55°C for 30 s, and 72°C for 30 s. Sequencing libraries were prepared according to the manufacturer's instructions of the NEBNext Ultra DNA Library Prep Kit for Illumina (New England Biolabs, Ipswich, MA, USA). The quantity of the libraries was verified using a Fluorometer (Qubit ® 4.0; Invitrogen, Carlsbad, CA, USA). Sequencing was conducted on an Illumina MiSeq PE250 platform using a paired-end protocol (Illumina Novaseq 6000 Miseq, USA; Meige Gene Technology Co. Ltd., Guangdong, China). Raw sequences were processed using the QIIME2 pipeline v.2020.8 (http://qiime.sourceforge.net/) [30], as described in Methods S2. The raw sequences have been submitted to the National Center for Biotechnology Information (NCBI, Bethesda, MD, USA) under the accession number PRJNA1001824.

Isolation and identification of wheat rhizosphere *bacteria*

The rhizosphere bacteria were isolated using high-throughput methods and their subsequent identification were performed according to previously reported protocols with certain modifications [31]. Rhizosphere bacteria were isolated using 96-well cell culture plates through a limiting dilution of the rhizosphere microbiota in liquid media, and the flowchart of rhizosphere bacterial isolation is shown in Fig. 1b. Briefly, 1.0 g of healthy plant rhizosphere soil from site 1 (cv. "LM 4," which is consistent with the wheat cultivar grown in the field in site 1) was added into 99.0 mL sterile phosphate buffer and homogenized at 180 r/min on a shaker [32]. Next, to enhance the diversity of the cultivated isolates and improve the efficiency of isolation, we employed the limiting dilution method by distributing soil suspension in liquid media across 96-well cell culture plates. The soil suspension was serially diluted with 10% tryptic soy broth (TSB) liquid medium to six different concentrations. Each diluent was aliquoted into a 96-well cell culture plate, with each well containing 200 µL suspension for cultivation. The concentration of diluted soil suspension that allows ~ 30% of the wells in a 96-well cell culture plate to show bacterial growth was selected as the optimal dilution concentration (ODC). At this concentration, most wells showing bacterial growth contain cultures originating from a single bacterial cell. After that, we diluted the soil suspension to the ODC by using 10% TSB liquid medium as well as 1/2 × ODC, and 2 × ODC to avoid experimental variation. Each diluent was aliquoted into 30 96-well cell culture plates, resulting a total of 8640 wells (3 diluents × 96 wells × 30 plates), with each well containing 200 µL suspension for cultivation. After a week of incubation, 3515 of the 8640 wells became turbid and showed bacterial growth. The cultures from these wells were preserved for future use by storing them in 30% glycerol at − 80°C. To identify the 16S rRNA gene sequences of these rhizosphere bacteria, a two-step barcode PCR scheme was employed, and the purified PCR products were sequenced on the Illumina MiSeq PE250 platform (Illumina Novaseq 6000 Miseq, USA; Meige Gene Technology Co. Ltd., Guangdong, China). After annotating the final sequence, the cultured bacteria were clustered into amplicon sequence variants (ASVs) using

(See figure on next page.)

Fig. 1 The workflow for this study. **a** The workflow for the field sampling. Sampling was conducted at three sites during the winter wheat seedling stage. At each site, we randomly collected samples from five plants from five healthy plots, five moderately diseased plots, and five severely diseased plots. For each plant, we collected its rhizosphere soil, roots, and leaves. These samples were used for microbial community analysis through 16S rRNA, ITS, and 18S rRNA gene amplicon sequencing. Furthermore, the rhizosphere soil samples were used for the determination of soil chemical properties and quantitative analysis of *Polymyxa graminis*. RNA was extracted from the leaves for quantitative analysis of wheat yellow mosaic virus (WYMV). At the ripening stage, we harvested all wheat plants and weighed the grain yield at the three sites. **b** Cultivation and identification of wheat rhizosphere bacteria and the isolation of *Sphingomonas azotifigens* and *Rhizobium deserti*. **c** The workflow of the hydroponic experiment. A WYMV-susceptible wheat cultivar (cv. "LM 4") was used for the hydroponic experiment. Before treatment, 24 wheat seedlings with similar growth were selected and transplanted into hydroponic boxes containing 1.0 L of sterilized 1/2 Hoagland nutrient solution. Four treatments were included in the experiment: control (sterile TSB solution), inoculation with *S. azotifigens* only (S), with of *R. deserti* only (R), and mixed inoculation with *S. azotifigens* and *R. deserti* (S + R). Ten milliliters of sterile TSB solution, R, S, and S + R bacterial suspensions (OD_{600} = 0.5) were inoculated into the sterilized 1/2 Hoagland nutrient solution every day for each treatment. After 7 days of cultivation, 12 plants from each treatment were infected with an equal amount of WYMV via root infection to serve as the infected group, and the remaining 12 wheat plants served as the uninfected control group. Plant samples were collected 14 days after WYMV infection. The height, fresh shoot and root weight, and root architecture of wheat seedlings were measured. The RNA of leaf samples was extracted for WYMV quantification and transcriptome analysis

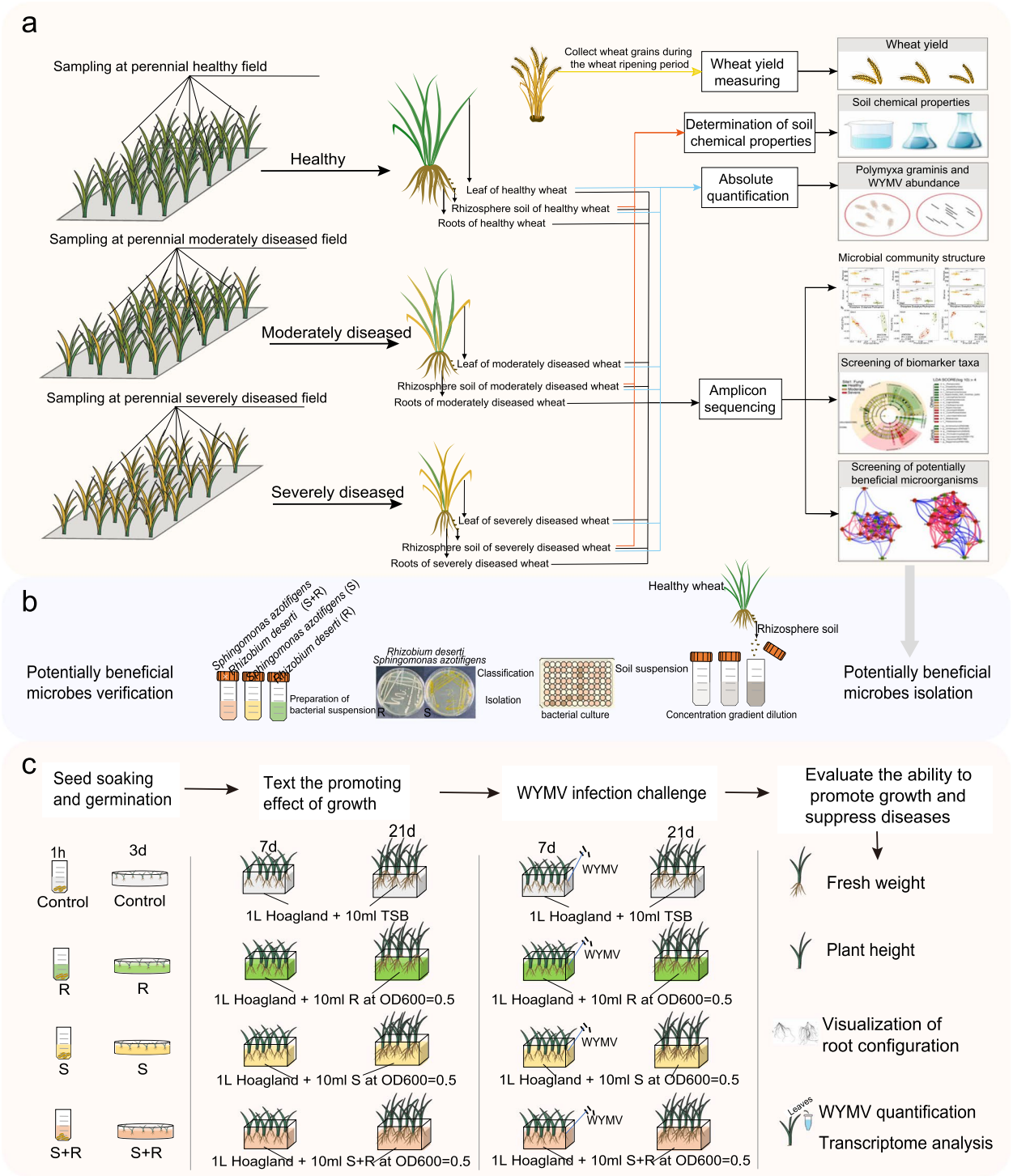

Fig. 1 (See legend on previous page.)

the QIIME2 pipeline v.2020.8 (http://qiime.sourceforge.net/). For each unique ASV, we selected 2–3 wells containing the corresponding bacteria and scratched the surface of the frozen bacterial culture with a pipette tip, followed by streaking them onto a 1/2 TSB plate. After purification, individual colonies were validated by Sanger sequencing using 27F and 1492R primers (Personalbio Technology Co., Ltd., Shanghai, China). We preserved

the bacteria when the Sanger sequencing results were consistent with the high-throughput sequencing results at − 80°C. MEGA 11.0.13 was used to construct phylogenetic trees.

Hydroponic experiment to assess the effects of *S. azotifigens* and *R. deserti* on wheat growth and defense against WYMV

A hydroponic experiment was carried out in a controlled growth chamber using a WYMV-susceptible wheat cultivar (cv. "LM 4," which is consistent with the wheat cultivar grown in the field in site 1). Four treatments were included in the experiment: control (sterile TSB solution), inoculation with *S. azotifigens* only (S), inoculation with *R. deserti* only (R), and mixed inoculation with *S. azotifigens* and *R. deserti* (S + R) (Fig. 1c). The bacterial suspensions were prepared as follows: we first inoculated each of the isolate onto a TSA plate. After 3–5 days of incubation, a single colony was picked from each plate and incubated in TSB liquid medium by shaking at 28°C at 180 rpm for 3–5 days. The bacterial suspensions were diluted into $OD_{600} = 0.5$ before use. Thirty seeds were used in each treatment, each containing three replicates. The selected wheat seeds were surface sterilized using the abovementioned approach. The surface-sterilized seeds were soaked in 10 mL of sterile TSB solution and S, R, or S + R bacterial suspensions ($OD_{600} = 0.5$) for an hour. Then, the seeds were germinated on sterilized moist filter paper in a glass garden at 30°C for 3 days. Twenty-four seedlings with similar growth were selected and transplanted into 6-well hydroponic boxes containing 1.0 L of sterilized 1/2 Hoagland nutrient solution [33]. Ten milliliters of sterile TSB solution and R, S, or S + R bacterial suspensions ($OD_{600} = 0.5$) were inoculated daily for each treatment throughout the hydroponic experiment (for 21 days). The nutrient solution was replaced every 3 days to maintain freshness and sufficient nutrients for plant growth. Seedlings were cultured in an artificial climate-controlled chamber at 18°C with 70% relative humidity and a 16 h:8 h light to dark cycle.

After 7 days of cultivation, 12 plants from each treatment were infected with an equal amount of WYMV virus through root infection (the infected group) and the remaining 12 wheat plants served as the uninfected control group. The steps for WYMV infection were as follows: (1) infected WYMV clones were constructed, (2) the wheat root surface was mildly scratched to create damage, (3) the roots were soaked in an *Agrobacterium* infiltration liquid ($OD_{600} = 0.5$) containing RNA1 and RNA2 infection clones, and (4) the soaked roots were placed in a vacuum pump for 30 min to allow *Agrobacterium* to invade the roots before returning them to the hydroponic system. The method for WYMV clone construction and root infection was the same as described previously [34]. After infection, the growth temperature was adjusted to 8℃ to optimize WYMV accumulation/infection. The uninfected control group received the same procedures as the infected ones (including root damage, soaking in an *Agrobacterium* infiltration liquid, and vacuum pumping), with the exception that the roots were soaked in the *Agrobacterium* without WYMV clones. Plant samples were collected 14 days after WYMV infection. The height and fresh shoot and root weights of the wheat seedlings were measured. The roots of each plant were scanned using a root scanner (WinRHIZO, 1,691,032–00, Japan) to visualize root architecture. Leaf samples from the same position on each plant were collected to extract total RNA for WYMV quantification and transcriptome analyses. A flowchart of the hydroponic experiment is shown in Fig. 1c.

RNA extraction, sequencing, and sequence processing

Total RNA was extracted from leaf samples in the abovementioned hydroponic experiment using the HiPure Plant RNA Mini Kit (Magen Biotechnology Co., Ltd., Guangzhou, China). The assessment of RNA quantity was conducted using a NanoDrop 2000 spectrophotometer (Thermo Fisher Scientific, USA). Libraries were prepared following the manufacturer's instructions of the VAHTS Universal V6 RNA-seq Library Prep Kit and sequenced on an Illumina Novaseq 6000 platform by OE Biotech, Inc. (Shanghai, China). The raw sequencing data have been deposited in the NCBI Short Read Archive (SRA) under the accession number PRJNA1039684. After sequencing, raw reads in FASTQ format were processed with fastp software and low-quality reads were eliminated to obtain clean reads [35]. Clean reads were mapped to the wheat reference genome using HISAT2 [36]. The calculation of fragments per kilobase per million mapped fragments (FPKM) for each gene was performed, and the read counts of each gene were acquired using HTSeq-count [37, 38]. In the present study, to confirm the RNA-seq results, four auxin and cytokinin pathway-related genes and four JA and SA pathway-related genes, which were significantly upregulated by *S. azotifigens* and *R. deserti*, were selected ($\log_2$ fold change at least > 1, $p < 0.05$). Their expression levels were determined by reverse transcription quantitative PCR (RT-qPCR). The detailed RT-qPCR procedure is described in Methods S1, and primer information is provided in Table S2.

Statistical analysis

All analyses were conducted using R software (v. 4.1.0) unless stated otherwise. We used the "ggpubr" package (v. 0.6.0) to test the differences in wheat yield and *P. graminis*

abundance between different disease severities using Student's *t*-tests. Pearson's correlation analysis was used to test for significant correlations between abundance of *P. graminis* and wheat yield. We used the "vegan" package (v. 2.6.4) to calculate the Shannon index and richness index alpha diversity of microbial communities, and principal component analysis (PCoA) based on the Bray–Curtis dissimilarity was used to characterize the beta diversity. LDA Effect Size analysis (LEfSe) (http://huttenhower.sph.harvard.edu/galaxy) was employed to identify genus-level microbial community biomarkers in the rhizosphere across varying disease severities (Kruskal–Wallis test, $p < 0.05$, log LDA score > 2.0) [39]. Biomarkers (at the genus level) were selected to construct correlation networks in rhizosphere soils based on Spearman correlations using the "igraph" (v. 2.0.3) and "reshape2" (v. 1.4.4) software packages. Each node symbolizes a biomarker, while each edge denotes a noteworthy correlation among biomarkers ($|r| > 0.6$, $p < 0.05$) [40]. The "randomForest" package (v. 4.7.1.1) was employed to assess the predictive performance of microbial communities in the rhizosphere soils, roots, and leaves (indicated by the richness, PCoA1 from the PCoA analysis, and the normalized abundances of the top 10 phyla from the bacterial, fungal, and protozoal communities) regarding grain yield and the abundances of WYMV and *P. graminis.* We also used the "randomForest" package (v. 4.7.1.1) to sort the top 10 biomarkers predicting the health status of winter wheat at each site based on the mean decreased accuracy [41]. Spearman's correlation analysis was used to test the significance of the correlation between the abundances of key biomarkers and soil chemical properties and wheat yield. The correlations were visualized with a heatmap using the "corrplot" (v. 0.92) and "Hmisc" (v. 5.1.2) packages [42]. The construction of the structural equation modeling (SEM) model was performed in AMOS 2.0 by using the robust maximum likelihood evaluation method [43]. Dominant biomarkers (indicated by the normalized abundances of the selected top 10 biomarkers), bacterial and fungal communities (indicated by the richness, PCoA1 from the PCoA analysis, and the normalized abundances of the top 10 phyla of bacterial and fungal communities), and soil edaphic properties (indicated by normalized soil properties) were used as variables for the SEM analysis. All variables were standardized using Statistical Product and Service Solutions (SPSS) software for model construction. Model fit was assessed using chi-square, *p* value, standardized residuals, root mean square error of approximation, and fit index.

To detect differentially expression genes (DEGs) across wheat plants according to the RNA-seq results, we used the DESeq2 method with a p value < 0.05 and fold change > 2 as the threshold [44]. Based on the hypergeometric distribution, Gene Ontology (GO) and Kyoto Encyclopedia of Genes and Genomes (KEGG) pathway enrichment analyses of the DEGs were performed to screen for significantly enriched terms [45, 46]. The "pheatmap" package (v. 1.0.12) was used to generate heatmaps illustrating gene expression in the pathways under different treatments.

Results

Correlating the plant-associated microbiome with wheat yield and the abundances of *P. graminis* and WYMV

The symptoms of wheat yellow mosaic disease in the field are shown in Fig. 2a. The onset of the wheat yellow mosaic disease caused yield losses of 15.8% ~ 29.3% at site 1, 15.1% ~ 19.6% at site 2, and 43.1% ~ 48.0% at site 3 (Fig. 2b). In general, the abundance of the viral vector *P. graminis* in the rhizosphere soil and the WYMV load in wheat leaves increased with the degree of disease in plants. Specifically, at stie 1, the abundance of *P. graminis* in the diseased rhizosphere increased by 101.5% ~ 306.5% compared with that in the healthy rhizosphere (Fig. 2c, d). The WYMV load increased from 0 in healthy plants, to 1.63×10^4 in moderately diseased plants, and to 1.28×10^6 in severely diseased plants. At site 2, the abundance of *P. graminis* in the diseased rhizosphere increased by 43.8% ~ 54.7% compared with that in the healthy rhizosphere. The WYMV load increased from 4.25×10^3 in healthy plants, to 6.32×10^3 in moderately diseased plants, and reached 3.35×10^7 in severely diseased plants. At site 3, the abundance of *P. graminis* in the diseased rhizosphere increased by 106.5% ~ 287.0% compared with that in the healthy rhizosphere, The WYMV load increased from 7.67×10^3 in healthy plants, to 1.61×10^6 in moderately diseased plants, and reached 6.75×10^6 in severely diseased plants. Consistently, we detected significant and strong negative correlations between the abundance of *P. graminis* ($R^2 = 0.61$, $p < 0.001$) in the wheat rhizosphere and WYMV load in wheat leaves ($R^2 = 0.41$, $p = 0.005$) and wheat yield across the three wheat fields. This suggested that the yield loss caused by wheat yellow mosaic disease was highly correlated with a higher WYMV load in leaves and an increased *P. graminis* abundance in the rhizosphere (Fig. 2e).

To reveal microbiome-mediated pathogen infection in wheat, we investigated the correlation of wheat yield, *P. graminis*, WYMV, and plant-associated microbiomes. We found that the microbial communities in the wheat rhizosphere exhibited better prediction performance for wheat yield, *P. graminis,* and WYMV than those in the roots and leaves. This indicated the important role of the rhizosphere microbiome in affecting grain yield and the occurrence of wheat yellow mosaic disease (Fig. 2f-h, Fig. S1-S3). Lastly, the bacterial and fungal communities

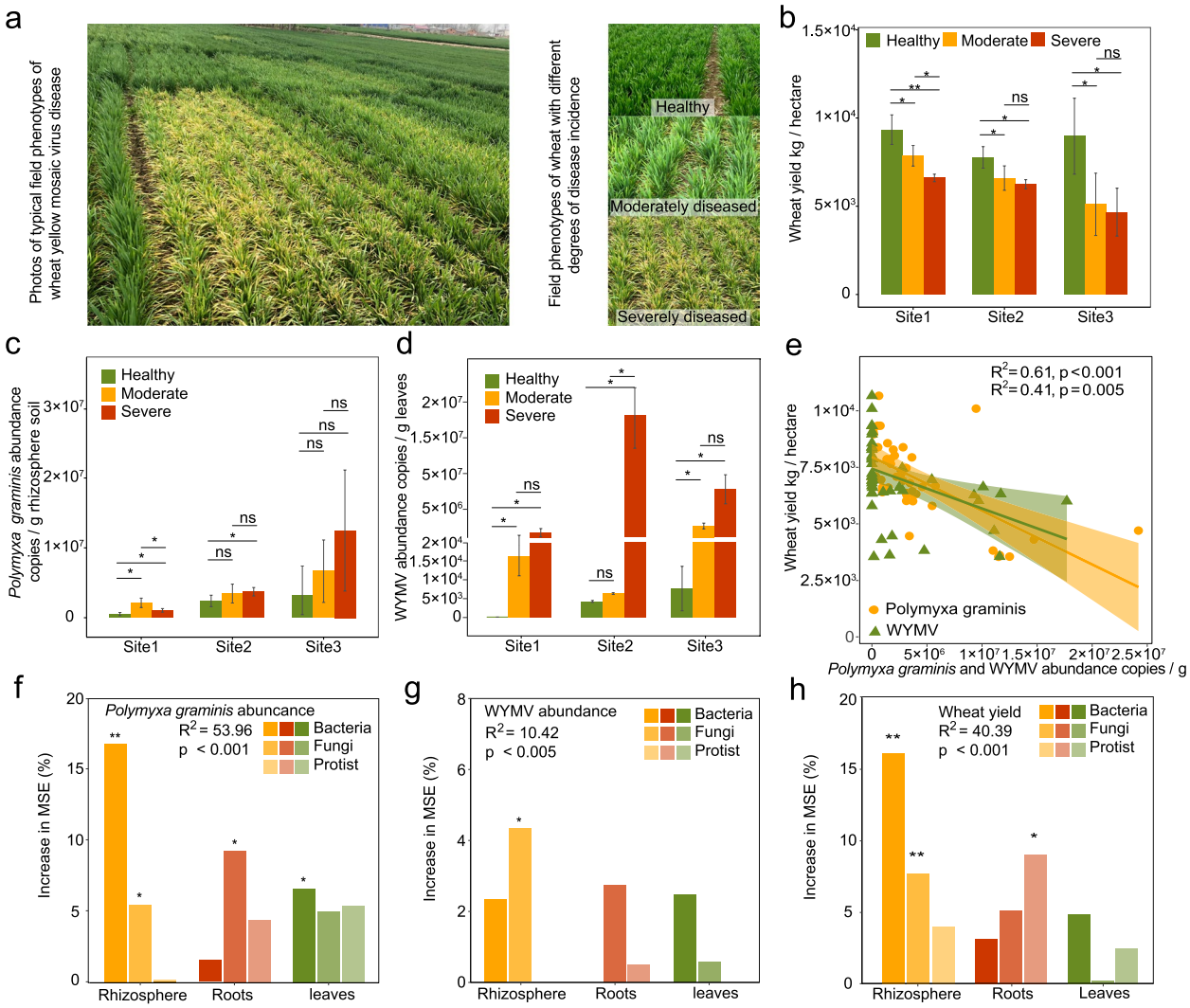

Fig. 2 Wheat yield, the abundance of *P. graminis* in wheat rhizosphere, the WYMV load in wheat leaves under different disease severities, and their correlation with plant-associated microbiomes. **a** Field phenotype of wheat yellow mosaic disease. **b** Wheat yield under different disease severities in Shandong (site 1), Jiangsu (site 2), and Henan (site 3). (c) The abundances of *P. graminis* in wheat rhizosphere under different disease severities at the three sites. **d** WYMV loads in wheat leaves under different disease severities at the three sites. Single and double asterisks indicate significant differences between healthy, moderately diseased, and severely diseased wheat plants at 1% and 5% levels (Student's *t*-test); ns no significant differences between healthy, moderately diseased, and severely diseased wheat plants at the 5% level (Student's *t*-test). The number of samples per replicate is five, and error bars represent standard deviations. **e** Correlations between the abundances of *P. graminis* in wheat rhizosphere, the loads of WYMV in wheat leaves and wheat yield. **f–h** The importance of bacterial, fungal, and protozoal communities in different wheat compartments for the prediction of *P. graminis* abundance, WYMV load, and wheat yield. Single and double asterisks indicate significance at 5% and 1% levels. Increase in MSE (%) means the percentage of increase of mean square error. A higher value of increase in MSE (%) indicates the more important of predictors

exhibited better predictive power for wheat yield, *P. graminis*, and WYMV than the protozoal community.

Community shifts in the rhizosphere microbiome under different disease severity

Based on the above results, our subsequent analyses concentrated on changes in bacterial and fungal communities within the wheat rhizosphere soil at three different disease severity levels. We observed a significant decrease in the Shannon index of bacterial and fungal communities in the rhizosphere of severely diseased plants compared to that of healthy plants at site 1 (Student's *t*-test, $p < 0.05$, Fig. S4a). Moreover, the community structure differed significantly among disease severities along the PCoA1 axis (bacterial community: $R^2 = 0.3467$, $p < 0.001$, ANOSIM; fungal community: $R^2 = 0.4773$,

$p < 0.001$, ANOSIM) at site 1 (Fig. S4b). No significant differences in alpha diversity and community structure were observed for either bacterial or fungal communities among different plant disease severities at site 2 and site 3 (Figs. S5, S6). In terms of alterations in the microbial community composition at the phylum level, the relative abundances of Bacteroidota and Ascomycota in the severely diseased rhizosphere decreased significantly compared to those in the healthy rhizosphere at site 1 and site 3, whereas Basidiomycota were significantly enriched in the severely diseased rhizosphere soils at all three sites (Fig. S4c-6c, Table S3-S4).

We then used LEfSe analysis to identify key bacterial and fungal taxa as biomarkers of wheat plant health status in the rhizosphere soil. We identified 15, 25, and 26 bacterial and fungal taxa as biomarkers at site 1, site 2, and site 3, respectively (Fig. 3a, Fig. S7a-S8a). In general, bacterial and fungal genera, including *Sphingomonas*, *Allorhizobium-Neorhizobium-Pararhizobium-Rhizobium*, *Umbelopsis*, *Burkholderia-Caballeronia-Paraburkholderia*, *Rokubacteriales*, *Pseudoxanthomonas*, *Filobasidium,* and *Tetracladium*, were identified as biomarkers in the healthy rhizosphere. Bacterial and fungal genera including *Pseudomonas*, *Tausonia*, *Fusicolla*, *Bipolaris*, *Stagonospora*, and *Thanatephorus* were identified as biomarkers of diseased rhizospheres.

To examine the correlations and potential competitive and cooperative relationships among the key biomarkers in the rhizosphere, we constructed co-occurring microbial networks for these biomarkers in healthy, moderately, and severely diseased rhizospheres. Intriguingly, the interactions between biomarkers in the healthy rhizosphere, exemplified by *Sphingomonas* and *Allorhizobium-Neorhizobium-Pararhizobium-Rhizobium,* demonstrated opposite correlations when compared to those in diseased plants, whether moderately or severely affected. Specifically, these correlations were negative in the healthy rhizosphere and positive in the diseased rhizosphere at site 1 (Fig. 3b). This suggests a transformative relationship, wherein these microbial taxa shift from being mutually exclusive in a healthy rhizosphere to becoming complementary and collaborative in a diseased state. Similar patterns were consistently observed in the key healthy wheat rhizosphere biomarkers at sites 2 and 3, where *Rokubactriales* and *Pedosphaerales* (at site 2) and *Filobasidium* and *Cyathus* (at site 3) exhibited distinct negative and positive patterns in the healthy and diseased rhizospheres, respectively (Fig. S7b, Fig. S8b).

The top biomarkers to predict the health status of wheat

Microbial biomarkers are crucial for early disease detection, yield prediction, quality assessment, environmental stress monitoring, breeding, optimizing resource use, and enhancing precision agriculture practices. Therefore, we next used a random-forest machine-learning approach to select the top 10 biomarkers at each site that could serve as key components to distinguish the healthy, moderately diseased, and severely diseased rhizospheres. Then we explored their correlations with soil chemistry, the abundances of *Polymyxa graminis* and WYMV, and wheat yield (Fig. 4a). Interestingly, we found that the top 10 biomarkers of the healthy rhizosphere were generally negatively correlated with soil organic carbon, soil available phosphorus, available potassium, and pH, whereas the biomarkers of the diseased rhizosphere showed a generally positive correlation with the available phosphorus, dissolved organic nitrogen, ammonium nitrogen, and nitrate nitrogen (Fig. 4b). Our in-depth analyses using the SEM showed that compared to soil chemical properties and microbial communities, microbial biomarkers and *P. gramins* abundances in the rhizosphere explained a larger effect size on wheat yield (Fig. 5b). That is, the microbial biomarkers not only had a direct positive correlation with wheat yield but also indirectly affected it by impacting the microbial communities and the abundance of *P. gramins* (Fig. 5a). These findings further demonstrated that microbial biomarkers in the rhizosphere play crucial roles in determining wheat yield by interacting with *P. gramins* in the rhizosphere.

Most of the biomarkers in the healthy rhizosphere, such as bacterial genera *Sphingomonas*, *Allorhizobium-Neorhizobium-Pararhizobium-Rhizobium*, *Mucilaginibacter, Burkholderia-Caballeronia-Paraburkholderia*, *Pseudoxanthomonas*, *Rokubacteriales,* and *Pedosphaeraceae* and fungal genera *Umbelopsis* and *Nigrospora*, were positively correlated with wheat yield across all three sites; on the contrary, the biomarkers in the diseased wheat rhizosphere soil, such as bacterial genera *Pseudomonas*, *Terrabacter,* and *Blastococcus*, and fungal genera *Tausonia, Naganishia*, *Fusicolla*, were all significantly negatively correlated with yield (Fig. 4b). Importantly, we found that *Sphingomonas* and *Allorhizobium-Neorhizobium-Pararhizobium-Rhizobium,* the key biomarkers in the healthy rhizosphere, not only exhibited substantial enrichment in the rhizosphere of healthy wheat plants but also had a positive correlation with wheat yield and a negative correlation with the abundance of WYMV. Collectively, these findings suggest that the two microbial taxa play a vital role in maintaining wheat health by conferring resistance against wheat yellow mosaic disease. This presents an intriguing avenue for further investigation to elucidate the underlying mechanisms of microbiome-mediated disease resistance in wheat plants.

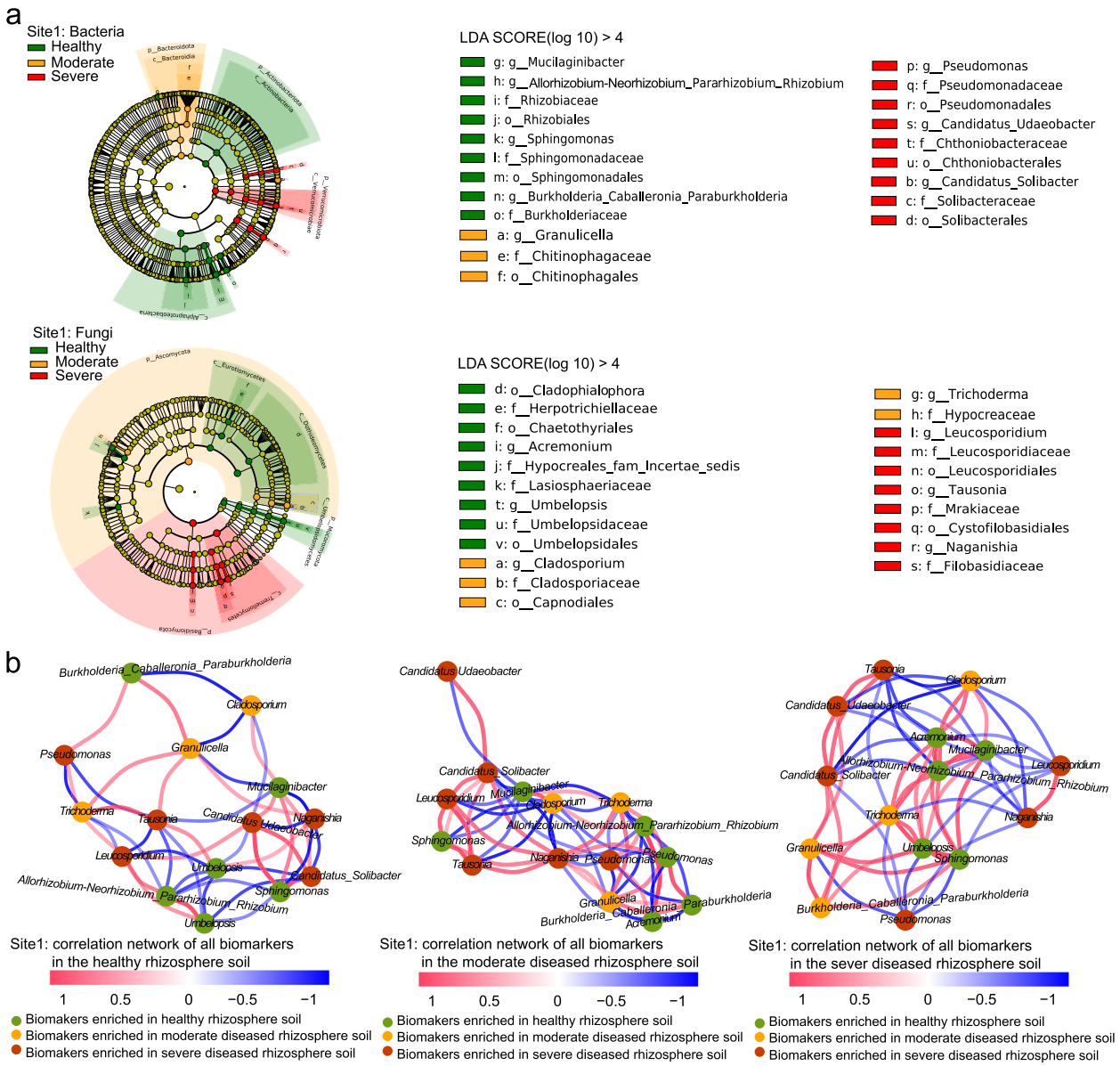

Fig. 3 Bacterial and fungal biomarkers in the healthy, moderately diseased, and severely diseased rhizospheres in Shandong (site 1) and their correlation networks. **a** The linear discriminant analysis effect size (LEfSe) analysis showing the significantly different bacterial and fungal taxa (biomarkers) among the different disease severities (LDA > 4 and $p < 0.05$). These taxa are symbolized by colored dots. From outside to inside, the five rings of the cladogram denote the phylum, class, order, family, and genus level, respectively. **b** Correlation networks of biomarkers in healthy, moderately diseased, and severely diseased rhizospheres ($|r| > 0.6$, $p < 0.05$). The color of each node represents the biomarkers (at the genus level) in healthy (green), moderately diseased (yellow), and severely diseased (red) rhizospheres. Red lines represent positive correlations, and blue lines represent negative correlations

Effects of *S. azotifigens* and *R. deserti* inoculations on wheat growth and defense against WYMV

To validate the growth-promoting and disease-defending capabilities of these two bacterial genera, *Sphingomonas* sp. and *Rhizobium* sp. were isolated from the rhizospheres of healthy wheat plants (cv. "LM 4") at site 1. We successfully isolated strains *S. azotifigens* from *Sphingomonas* and *R. deserti* from the *Allorhizobium-Neorhizobium-Pararhizobium-Rhizobium*. To verify that *S. azotifigens* and *R. deserti* were indeed enriched in the healthy rhizosphere, we compared the abundances of all ASVs affiliated with these genera across healthy, moderately diseased, and severely diseased rhizospheres (Fig. S9). We also constructed phylogenetic trees

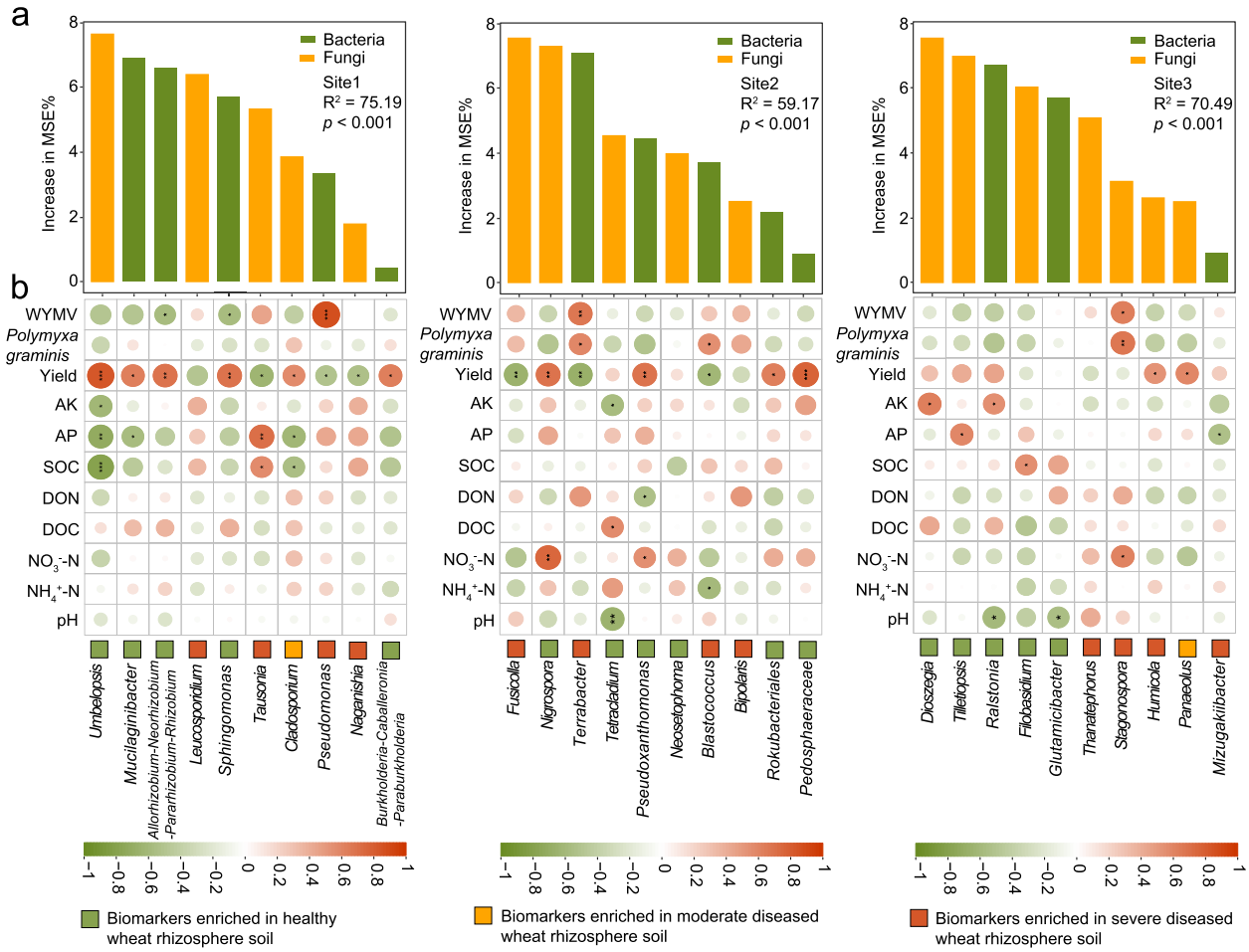

Fig. 4 The top 10 biomarkers for the healthy, moderately diseased, and severely diseased rhizospheres, and their correlations with soil chemical properties, *P. graminis* abundance, WYMV load and wheat yield. **a** The top 10 biomarkers that can be used to distinguish the healthy, moderately diseased, and severely diseased rhizospheres at each sampling site. Increase in MSE (%) means the percentage of increase of mean square error. A higher value of increase in MSE (%) indicates the more important of predictors. **b** The correlations between the relative abundances of the top 10 biomarkers and soil chemical properties, *P. graminis* abundance, WYMV load and wheat yield. Single, double, and triple asterisks indicate significance at 5%, 1% and 0.1%, respectively (Spearman correlations)

using representative sequences from these ASVs alongside sequences from our isolates. We found that the sequences of *S. azotifigens* and *R. deserti* matched those of ASV195 and ASV48, respectively, with 100% accuracy. Furthermore, the abundances of ASV195 and ASV48 were significantly higher in the healthy rhizosphere compared to the diseased rhizospheres, suggesting that these two isolates correspond to ASV195 and ASV48 and were indeed enriched in the healthy rhizosphere.

A hydroponic experiment was conducted to investigate the effects of these two isolates on wheat plant growth and disease resistance. Our results showed that plant height (~12%), shoot biomass (~11%), root diameter (~15%), and root volume (~35%) were significantly improved by co-inoculation with *S. azotifigens* and *R. deserti* compared to the control, regardless of WYMV infection ($p < 0.05$, Fig. 6a, Fig. S10). Moreover, the abundance of WYMV decreased by ~83% ($p < 0.01$) after inoculation with *S. azotifigens* alone or co-inoculation with *S. azotifigens* and *R. deserti* compared to the control (Fig. 6b).

RNA sequencing was used to investigate the mechanisms by which *S. azotifigens* and *R. deserti* benefit wheat growth and disease tolerance (Fig. S11-S12). We found that when *S. azotifigens* and *R. deserti* were inoculated, genes within the auxin and cytokinin pathways, including auxin (AUX), indole-3-acetic acid (IAA), auxin response factor (ARF), cytokinin receptor (CRE1), and Arabidopsis response regulator (ARR) protein coding genes were significantly upregulated compared with the control

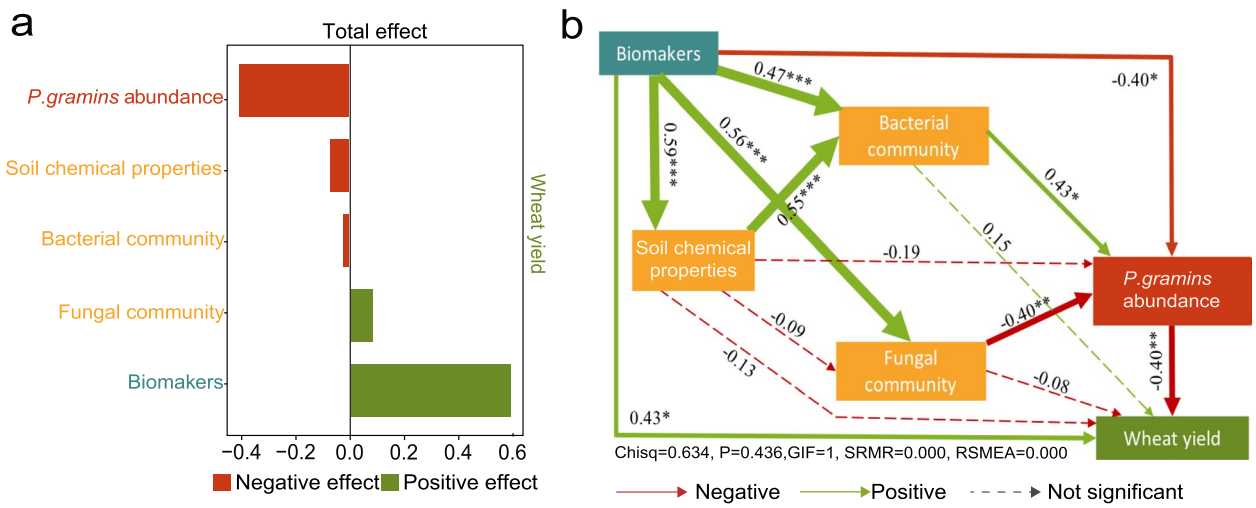

Fig. 5 The effects of the biomarkers, soil microbial communities, soil chemical properties, and *P. gramins* abundance in wheat rhizosphere on wheat yield. **a** Standardized total effect of the biomarkers, soil microbial communities, soil chemical properties, and abundance of *P. gramins* in wheat rhizosphere on wheat yield. **b** The structural equation model showing the relationship between the biomarkers (indicated by the normalized abundances of the top 10 biomarkers), soil microbial communities (indicated by the richness, PCoA1 of the PCoA analysis, and the normalized abundances of the top 10 bacterial and fungal phyla), soil chemical properties, and abundance of *P. gramins* in wheat rhizosphere and wheat yield. Solid arrows indicate significant impacts, while dotted arrows indicate non-significant impacts. Green lines indicate positive impacts, and red lines indicate negative impacts. The width of the arrow represents the strength of the significantly standardized path coefficient. Single, double, and triple asterisks indicate significance at 5%, 1%, and 0.1%, respectively

in the uninfected group ($\log_2$ fold change at least > 2, $p < 0.05$). Genes involved in the JA and SA pathways, including transcription activation factor (MYC2) and pathogenesis-related protein (PR-1)-related genes, were significantly upregulated ($\log_2$ fold change at least > 2, $p < 0.05$) following inoculation with *S. azotifigens* and *R. deserti* compared to the control in the WYMV-infected group (Fig. 7a).

RT-qPCR further confirmed the RNA-seq results (Fig. 7b). For example, the expression levels of *TraesCS4B02G161800* (related to ARF), *TraesCS6B02G027800*, *TraesCS3A02G275400*, and *TraesCS3802G309100* (related to CRE1) were significantly upregulated ($\log_2$ fold change at least > 1, $p < 0.05$) following inoculation with *S. azotifigens* and *R. deserti* compared to the control in the uninfected group. The expression of *TraesCS1A02G193200* (related to MYC2) was significantly upregulated ($\log_2$ fold change at least > 1, $p < 0.05$) following inoculation with *R. deserti*, and those of *TraesCS5B02G442600*, *TraesCS5D02G446900*, and *TraesCS5B02G442700* (related to PR-1) were significantly upregulated ($\log_2$ fold change at least > 1, $p < 0.05$), especially following inoculation with *S. azotifigens* alone or mixed inoculation with *S. azotifigens* and *R. deserti* in the WYMV-infected group. These results demonstrated that inoculation with *S. azotifigens* and *R. deserti* improved the growth of wheat seedlings, mainly by enhancing the auxin and cytokinin pathways and suppressing WYMV infections by activating plant defense signalling (e.g., JA and SA).

Discussion

The rhizosphere microbiome is an effective predictor for WYMV infection and wheat yield

Previous studies on wheat yellow mosaic disease have focused on the interaction between WYMV and host plants [15, 47]; however, soil processes, especially the relationship between WYMV, *P. graminis* (the vector of WYMV), and soil microbiomes, have been largely ignored. In the present study, the *P. graminis* abundance in the rhizosphere increased with the disease severity and was negatively correlated with wheat yield. This suggests the possibility of predicting the onset of wheat yellow mosaic disease and wheat yield by monitoring dynamic changes in *P. graminis* in the rhizosphere as an additional and promising approach, alongside traditional measurements of WYMV load in leaves. We found that compared with the microbial communities in the roots and leaves of wheat, the rhizosphere microbiome was more predictive of wheat yield and the abundances of *P. graminis* and WYMV. This indicates that the rhizosphere is the most important hotspot for crosstalk between WYMV, *P. graminis*, microbiomes, and host plants. Although the rhizosphere microbiome is acknowledged as the first line of defense against soil-borne pathogens, encompassing bacteria, fungi, nematodes, etc. [48] and plays important roles in crop productivity [49], our study highlights the importance of the rhizosphere microbiome in response to soil-borne viral infections in wheat plants. This may be because, during the period when

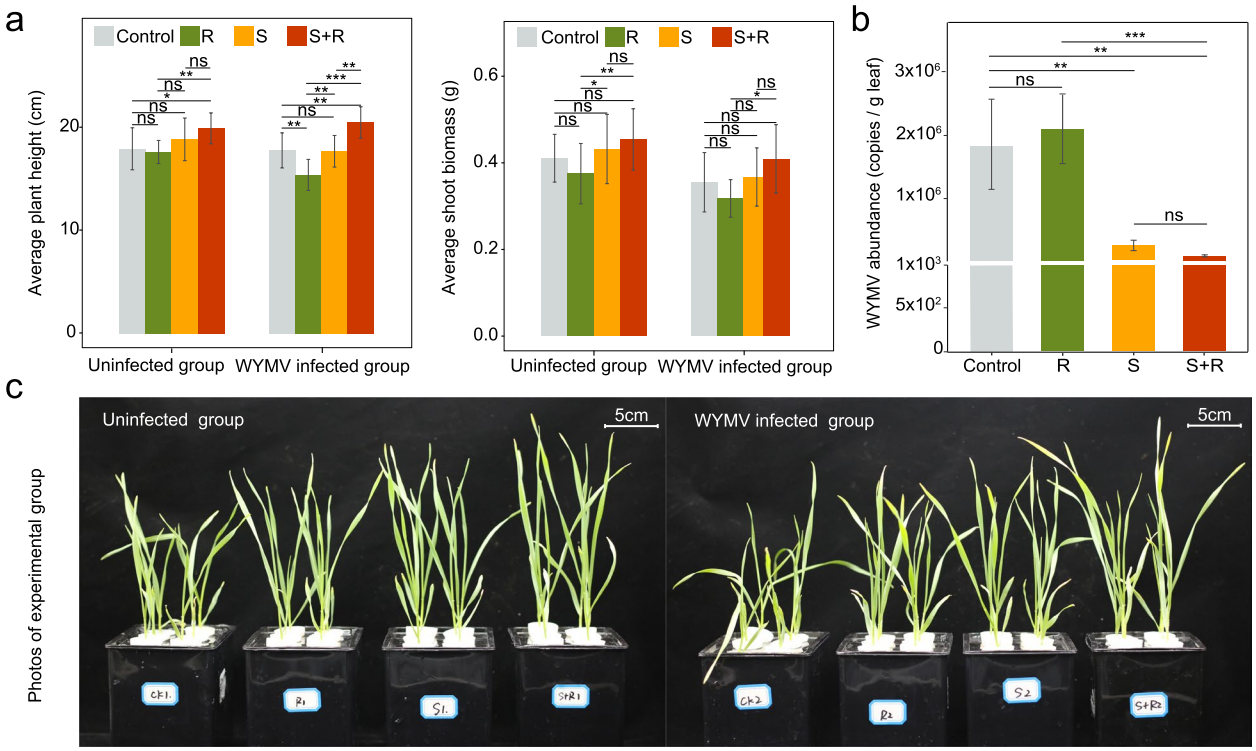

Fig. 6 The effect of potentially beneficial strains (*R. deserti* and *S. azotifigens*) on wheat growth and WYMV resistance. **a** Average plant height and shoot biomass of wheat following inoculation with *S. azotifigens* only (S), *R. deserti* only (R), or both *S. azotifigens* and *R. deserti* (S + R) in the WYMV-infected and uninfected experimental groups. **b** The WYMV loads in leaves under the S, R and S + R treatments after 14 days of WYMV infection. Single, double, and triple asterisks indicate significant differences between treatments at 5%, 1%, and 0.1%, respectively (Student's *t*-test). ns no significant differences between treatments at the 5% level (Student's *t*-test). The number of samples per replicate was 12, and error bars represent standard deviations. **c** Images of wheat plants in the infected and uninfected groups (taken 14 days after WYMV infection)

the zoospores of the *P. graminis*, which carry the WYMV move from the soil to the rhizosphere, they have to compete with the indigenous rhizosphere microorganisms for space and nutrients. This process will induce significant alteration in rhizosphere microbial communities and influence the outcome of WYMV infection [50]. These findings also suggest that investigating changes in the rhizosphere microbiome under soil-borne viral infections and identifying the key rhizosphere microbial taxa that respond to the infection can offer novel opportunities for implementing preventive measures to control soil-borne viral diseases, thus improving crop yields.

Healthy rhizospheres are enriched with beneficial microorganisms while diseased rhizospheres are associated with a pathobiome that facilitates WYMV infection

Deciphering biomarker taxa and their correlations with host health status is crucial for utilizing plant microbiomes to boost both plant growth and overall health. This study found that the biomarkers of healthy rhizospheres at the three experimental sites were primarily plant growth-promoting and biocontrol microorganisms. For example, *Burkholderia-Caballeronia-Paraburkholderia* has the ability to antagonize root rot pathogens [51]. *Allorhizobium-Neorhizobium-Pararhizobium-Rhizobium* and *Rokubacteriales* are typical plant growth-promoting bacteria with nitrogen fixing abilities [52, 53]. *Sphingomonas* spp. are bacteria known for promoting plant growth by producing gibberellins and indole-3-acetic acid (IAA) [54, 55]. *Umbelopsis isabelline* has the ability to inhibit the virulence of chestnut blight cankers [56]. *Tetracladium* spp. positively influence the health and growth of their hosts and are positively associated with rapeseed yield [57]. *Filobasidium capsuligenum* has been found to promote grape ripening [58]. *Tilletiopsis pallescens* is an antagonist of the fungal pathogen *Erysiphe graminis* [59].

Unlike microbial biomarkers in healthy rhizosphere soils, diseased rhizosphere soils harbored an increased presence of pathobiomes and saprophytic fungi. For example, the genus *Pseudomonas*, which includes typical pathogens that thrive in moist environments, was also detected as a biomarker of the diseased wheat

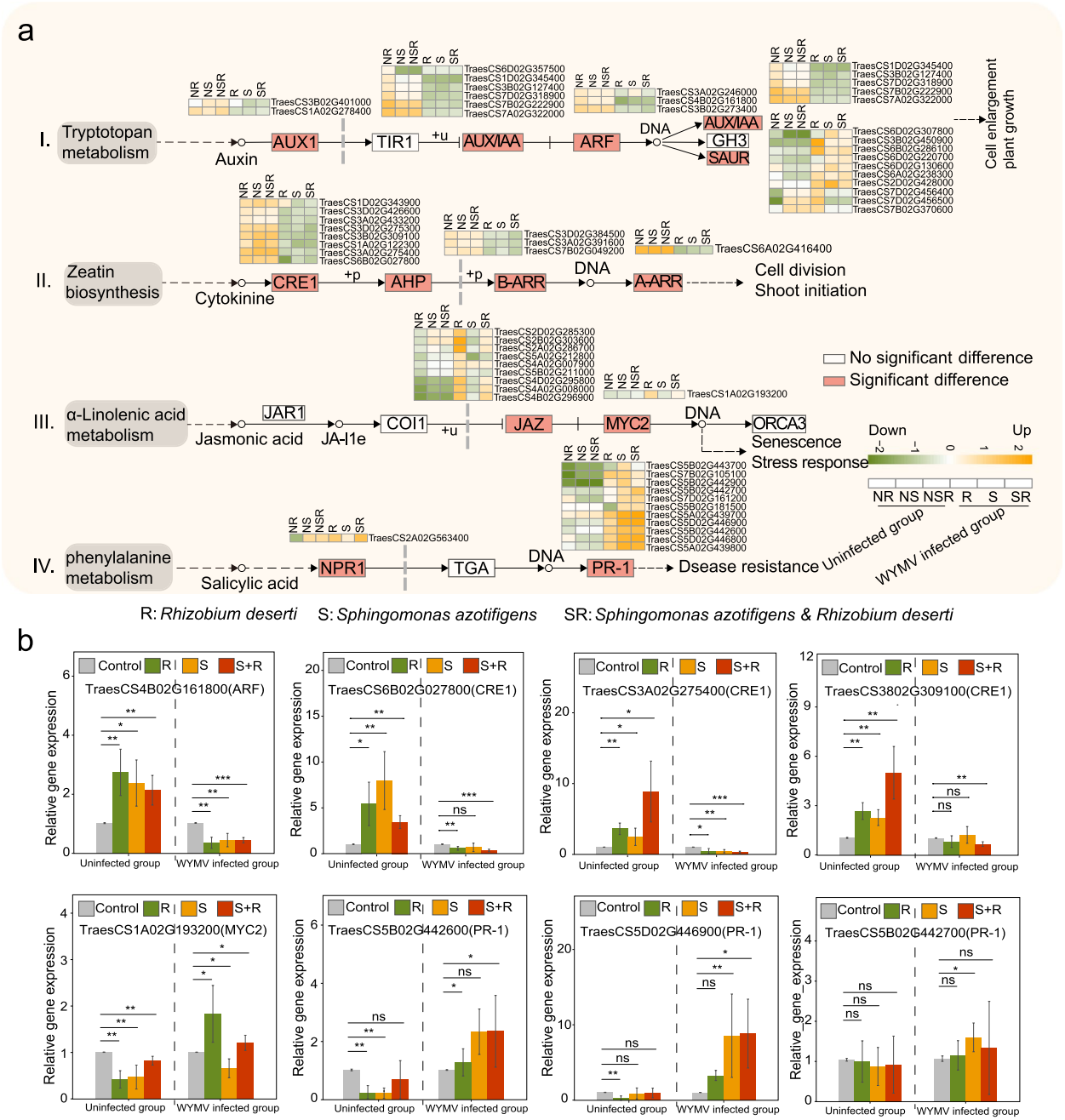

Fig. 7 Gene profiling of wheat plants with and without the inoculation of bacterial isolates or WYMV infection treatments. **a** Plant hormone signal transduction pathways (I. Auxin signaling pathway; II. Cytokinin signaling pathway; III. Jasmonic acid signaling pathway; IV. Salicylic acid signaling pathway). Heat maps showing the logarithmic fold change of differentially expression genes (DEGs) in all the treatments relative to control. NR, NS, and NSR indicate inoculation with *R. deserti* only, *S. azotifigens* only, or both *S. azotifigens* and *R. deserti* in the uninfected group, respectively; R, S, and SR indicated inoculation with *R. deserti* only, *S. azotifigens* only, or both *S. azotifigens* and *R. deserti* in the WYMV-infected group, respectively. **b** Relative expression levels of genes involved in plant hormone signal transduction. Single, double, and triple asterisks indicate significant differences between treatments at 0.1%, 1%, and 5%, respectively (Student's *t*-test). ns no significant difference between treatments at the 5% level (Student's *t*-test). The number of samples per replicate is 12, and error bars represent standard deviations

plants, negatively correlating with wheat yield in our study [60]. Some species in the genus *Tausonia* are primarily implicated in the mold rot of many substances [61]. *Naganishia* spp. have been reported to compete with plants for nutrients [53], while *Fusicolla* spp. are typical pathogenic fungi affecting several crops [6, 62].

Additionally, *Bipolaris maydis* causes southern corn leaf blight [63], and *Stagonospora nodorum*, a prominent necrotrophic pathogen in wheat, induces *Stagonospora nodorum* leaf and glume blotches [64]. *Thanatephorus cucumeris* is a broad-host-range pathogen that induces diseases such as blast root rot and standing blight [65]. Previous studies have also shown that certain potential pathogenic microbes demonstrated synergistic effects that exacerbate diseases [8], and diseased plants show an increased susceptibility to further colonization by pathogenic fungi [66]. For example, several potential pathogenic fungi from genera *Diaporthe*, *Fusarium*, *Phomopsis*, *Plectosphaerella*, *Stemphylium*, and *Cryptococcus* were enriched in plants afflicted with the Fusarium wilt [66]. Furthermore, pathobiomes can facilitate the pathological processes in host plants of the pathogens by attenuating the plant resistance [67]. For instance, the vitamin B6 produced by *Fusarium equiseti* promoted *Phytophthora sojae's* infection on soybean plants [68]. Similarly, in our study, we assumed that the colonization of these potential pathogenic fungal species and *P. graminis* may have mutually promoted their growth and colonization on plants, thereby increasing the accumulation of WYMV and exacerbating symptoms of wheat yellow mosaic disease.

The present study did not find an obvious enrichment of beneficial microbes in the diseased rhizosphere, which is different from previous studies showing that host plants recruit growth-promoting and biocontrol microbes to the rhizosphere to suppress soil-borne pathogens [69, 70]. This could be attributed to the nature of the virus-caused disease investigated in this study, the specific soil types, and the wheat varieties used. Not all soil-borne diseases or crop varieties employ a strategy akin to a cry for help to cope with pathogens. Additionally, we collected samples at the initial stage of infection rather than at a later stage, which might not have allowed for significant accumulation of beneficial microbes that tend to occur at later stages. Instead, we observed that the beneficial bacterial genera *Sphingomonas* and *Allorhizobium-Neorhizobium-Pararhizobium-Rhizobium* competed with each other in the healthy rhizosphere and cooperated with each other in the diseased rhizosphere. This may be because, compared to the healthy rhizosphere, there was less niche competition and more complementary use of resources between these two beneficial bacteria in the diseased rhizosphere [71]. When a pathogen invades, *Sphingomonas* and *Allorhizobium-Neorhizobium-Pararhizobium-Rhizobium* in the rhizosphere may work together to resist infections. Similarly, other beneficial bacteria, including *Pseudomonas* spp. and *Bacillus* spp., have been acknowledged to coexist and cooperate in the diseased rhizosphere [70].

S. azotifigens and R. deserti promote wheat disease resistance by activating plant hormone signaling pathways

Based on our hydroponic experiment, we found that inoculation with *S. azotifigens* alone and co-inoculation with *S. azotifigens* and *R. deserti* promoted wheat growth and inhibited WYMV infection, providing direct evidence that key beneficial microbes in the rhizosphere maintain plant health and help plants resist viral infections. The effects of inoculation with beneficial microbes on plant growth and disease resistance have been reported [72, 73]. A previous study reported that inoculation of *Sphingomonas* sp. Cra20 and *Pseudomonas putida* KT2440 resulted in a downregulation of virulence-related genes of the pathogen *Ralstonia solanacearum* and increased plant resistance to tomato bacterial wilt [72]. Another study showed that co-inoculation with beneficial rhizobacteria and rhizobium *Sinorhizobium meliloti* markedly elevated the nutrient (N, P, and K) content of plants and induced the release of secondary metabolites that promote nutrient uptake or inhibit rhizosphere plant pathogens [73]. Although the growth-promoting and pathogenic microorganism-inhibiting effects of beneficial microbes have been studied previously, our study, for the first time, demonstrated that rhizospheric colonization by key beneficial microbes can effectively help hosts resist viral infection and thus prevent viral diseases.

Recent experimental frameworks indicated that the mechanisms underlying the improved host defense against pathogens facilitated by colonization by beneficial microbes were as follows: (1) ISR of the host, which is mediated by JA and ethylene [73, 74]; (2) inducing metabolic defense in a host branched-chain amino acid-dependent manner [75]; (3) generating enzymes to scavenge reactive oxygen species in the host [76]; and (4) enhancing nutrient uptake, improving plant root structure, and promoting root cell wall thickening, fibrosis, and lignification [77]. In the present study, the growth-promoting and disease-inhibiting effects mediated by beneficial bacteria were mainly related to plant hormone signaling pathways. We found that in the uninfected experimental group, inoculation with potentially beneficial bacteria promoted the growth of wheat mainly through the significant upregulation of genes involved in the auxin and cytokinin signaling pathways, which is consistent with previous studies [24, 78, 79]. In the WYMV-infected group, these beneficial bacteria interacted closely with the host immune system and reduced the abundance of WYMV, mainly by activating the JA and SA pathways. Similarly, previous studies have indicated that beneficial bacteria and fungi, including *Stenotrophomonas*, *Penicillium*, *Pseudomonas*, *Streptomyces*, and *Trichoderma*, significantly activate JA- and SA-related pathways and improve the disease resistance

of host plants [62, 74]. SA-dependent systemic acquired resistance and JA-dependent ISR pathways are important components of plant defense transduction networks against pathogen attack.

The role of the JA and SA pathways in resisting pathogenic microorganisms and insects has been fully studied, that is, the JA-dependent pathway regulates resistance against necrotrophic pathogens and insects, whereas the SA-dependent pathway regulates resistance against biotrophic pathogens [80]. However, whether these two pathways are involved in plant antiviral immunity, especially anti-WYMV, has not been as extensively studied. Recent studies confirmed the significant role of the JA and SA pathways in viral resistance and demonstrated that JA signaling collaborates with the brassinosteroid, abscisic acid, and auxin pathways to induce antiviral immunity in rice [81–83]. In terms of the SA pathway, the hypersensitivity-induced reaction gene (HIR3) governs plant resistance against rice stripe virus (RSV) infection through a salicylic acid (SA)-dependent pathway in rice [84]. Additionally, the sulfotransferase STV11, responsible for converting SA to sulfonated SA, provides enduring resistance to rice stripe virus (RSV) [85]. We speculate that microbe-induced activation of the JA and SA pathways may protect wheat plants against WYMV infection through the above mechanisms. It should be noted that this study verified the plant growth-promoting and disease-inhibiting effects of beneficial bacteria under hydroponic conditions for only a short time, and a longer period of plant growth and disease suppression is needed to reveal whether the activation of plant defense is long-lasting.

The findings of our study hold significant potentials for applications in agricultural settings aimed at controlling soil-borne viral diseases. The utilization of microbial inoculants containing beneficial bacteria and their metabolites can be used to modulate the rhizosphere microbiome in disease-prone areas. The inoculants and their effective metabolic components can be developed into probiotics and postbiotics that combat viral diseases

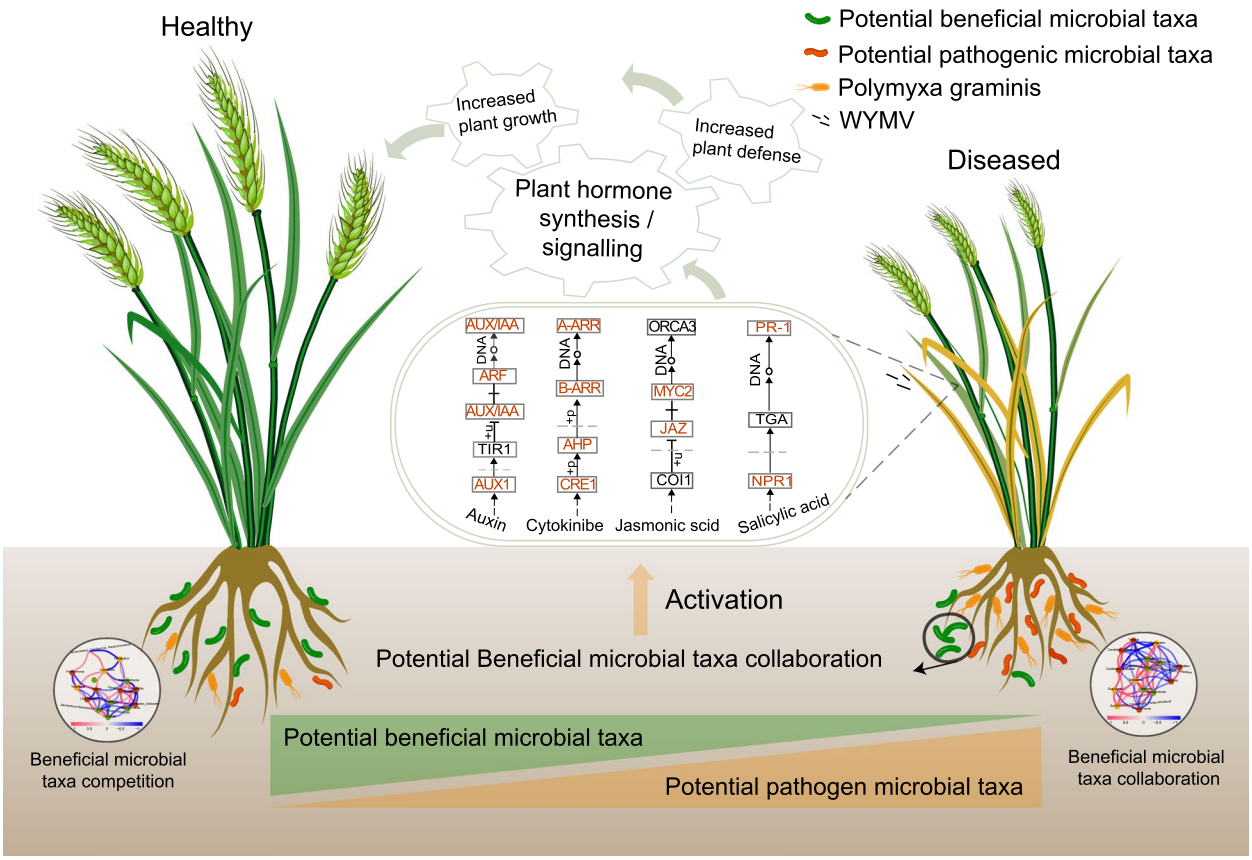

Fig. 8 Schematic diagram demonstrating the main results of the present study. Healthy rhizospheres were marked by the presence of putative beneficial microorganisms, while diseased ones were associated with a pathobiome characterized by a higher presence of putative pathogens. Beneficial microbial taxa competed with each other in the healthy rhizosphere but cooperated with each other in the diseased rhizosphere. These beneficial microorganisms can promote plant growth and increase wheat disease resistance by activating plant hormone signaling pathways, including cytokinin signaling, jasmonic acid signaling, and salicylic acid signaling

in fields. Additionally, by gaining a deeper understanding of factors influencing the rhizosphere microbiome, particularly the activities of the virus vector *P. graminis* zoospores, farmers can effectively reduce the prevalence of soil-borne diseases and sustain crop yields. However, it is crucial to conduct large-scale field tests to evaluate their effectiveness across different climate and soil conditions, as well as to assess any potential environmental hazards. Future studies could also investigate how multitrophic interactions between protists, bacteria, and fungi are influenced by the viral disease infection through analysis and integration of the current datasets, for example, using co-occurrence network analyses. Moreover, it would be interesting to explore the underlying mechanisms of the vector–virus relationship, including how the soil/plant microbiome influences these associations.

Conclusions

In this study, we explored the microbial community within the plant–soil system under healthy, moderately diseased, and severely diseased conditions across the main regions affected by wheat yellow mosaic and their relationships with WYMV, *P. gramins*, and wheat yield. Our results highlight the significance of the rhizosphere microbiome in the response to soil-borne viruses and their contribution to wheat yield. Furthermore, we identified biomarkers enriched in healthy rhizospheres, which are beneficial microbes that work together to resist pathogens and maintain plant health. We provide evidence that these beneficial microbes isolated from the wheat rhizosphere promote wheat growth by activating the auxin and cytokinin signaling pathways, while inhibiting WYMV infection by stimulating the JA and SA pathways (Fig. 8). These findings offer an alternative approach to control soil-borne viral diseases and maintain crop production by leveraging beneficial microbes to outcompete or inhibit the growth of pathogens.

Supplementary Information

The online version contains supplementary material available at https://doi.org/10.1186/s40168-024-01911-z.

Additional file 1: Methods S1. Real-time quantitative PCR. Methods S2. 16S rRNA, ITS and 18S rRNA genes amplicon sequencing data processing. Table S1. Detailed sampling information. Table S2. Primer sequences used in this study. Table S3. The relative abundances of major bacterial phyla in the rhizosphere of healthy, moderately and severely diseased wheat plants. Table S4. The relative abundances of major fungal phyla in the rhizosphere of healthy, moderately and severely diseased wheat plants. Fig. S1. Richness index of bacterial, fungal and protozoal communities in different wheat compartments (rhizosphere, roots and leaves) under the healthy, moderately and severely diseased conditions collected from Shandong (Site1), Jiangsu (Site 2) and Henan (Site 3). *, ** and *** indicate significant differences between healthy, moderately diseased and severely diseased wheat at 1% and 0.1% level, respectively (Student's *t*-test). ns indicates no significant difference (Student's *t*-test). Fig. S2. Principal coordinates analysis (PCoA) of the bacterial, fungal, and protozoal communities in different wheat compartments (rhizosphere, roots and leaves) under the healthy, moderately and severely diseased conditions collected from Shandong (Site1), Jiangsu (Site 2) and Henan (Site 3). Fig. S3. Relative abundance of the major phyla in the bacterial, fungal and protozoal communities in different wheat compartments (rhizosphere, roots and leaves) under the healthy, moderately and severely diseased conditions collected from Shandong (Site1), Jiangsu (Site 2) and Henan (Site 3). Fig. S4. Differences in diversity and structure of bacterial and fungal communities in wheat rhizosphere soil under different disease severities at Shandong (site1). (a) Shannon index of bacterial and fungal community. * and** indicate significant differences between healthy, moderately and severely diseased wheat plants at 5% level and 1% level (Student's *t*-test). ns, indicates no significant differences between healthy, moderate and severe diseased wheat plants at a 5% level (Student's *t*-test). (b) Principal coordinates analysis (PCoA) of bacterial and fungal communities. (c) Relative abundance of the major phyla in the bacterial and fungal community (top 10). Fig. S5. Differences in diversity and structure of bacterial and fungal communities in wheat rhizosphere soil under different disease severities at Jiangsu (site2). (a) Shannon index of bacterial and fungal community. ns, indicates no significant differences between healthy, moderate and severe diseased wheat plants at a 5% level (Student's *t*-test). (b) Principal coordinates analysis (PCoA) of bacterial and fungal communities. (c) Relative abundance of the major phyla in the bacterial and fungal community (top 10). Fig. S6. Differences in diversity and structure of bacterial and fungal communities in wheat rhizosphere soil under different disease severities at Henan (site3). (a) Shannon index of bacterial and fungal community. ns, indicates no significant differences between healthy, moderate and severe diseased wheat plants at a 5% level (Student's *t*-test). (b) Principal coordinates analysis (PCoA) of bacterial and fungal communities. (c) Relative abundance of the major phyla in the bacterial and fungal community (top 10). Fig. S7. Bacterial and fungal biomarkers in healthy, moderately and severely diseased rhizosphere soil in Jiangsu (Site2) and their correlation networks. (a) The linear discriminant analysis effect size (LEfSe) analysis showed the significantly different taxa of bacterial and fungal communities (biomarkers) among different disease severities (LDA > 2 and $p < 0.05$). These taxa are symbolized by colored dots. From outside to inside, the five rings of the cladogram denote the phylum, class, order, family, genus, respectively. (b) Correlation networks of biomarkers in healthy, moderately and severely diseased rhizosphere ($|r| > 0.6$, $p < 0.05$). The color of each node represents the biomarkers (at genus level) in healthy (green), moderately diseased (yellow) and severely diseased (red) rhizosphere. Red lines represent positive correlations, and blue line represents negative correlations. Fig. S8. Bacterial and fungal biomarkers in healthy, moderately and severely diseased rhizosphere soil in Henan (Site3) and their correlation networks. (a) The linear discriminant analysis effect size (LEfSe) analysis showed the significantly different taxa of bacterial and fungal communities (biomarkers) among different disease severities (LDA > 3 and $p < 0.05$). These taxa are symbolized by colored dots. From outside to inside, the five rings of the cladogram denote the phylum, class, order, family, genus, respectively. (b) Correlation networks of biomarkers in healthy, moderately and severely diseased rhizosphere ($|r| > 0.6$, $p < 0.05$). The color of each node represents the biomarkers (at genus level) in healthy (green), moderately diseased (yellow) and severely diseased (red) rhizosphere. Red lines represent positive correlations, and blue line represents negative correlations. Fig. S9.The relative abundances ofASVs affiliated to the genera *Allorhizobium-Neorhizobium-Pararhizobium-Rhizobium* (a) *and Sphingomonas* (b). Phylogenetic trees using the representative sequences of the ASVs affiliated to the genera *Sphingomonas* and *Allorhizobium-Neorhizobium-Pararhizobium-Rhizobium*and the sequences of *Sphingomonas azotifigens* (c) and *Rhizobium deserti* (d) (isolated from the healthy wheat rhizosphere at site 1). Names colored in blue indicate the isolates, and those colored in red indicate the ASV whose representative sequence matched 100% with the isolates. Fig. S10. Root system architecture under the inoculation of *S. azotifigens* only (S), *R. deserti* only (R), and co-inoculation of *S. azotifigens* and *R. deserti* (S+R) in the wheat yellow mosaic virus (WYMV) uninfected experimental group. (a) Root biomass, Root length, average root

diameter, and total root volume obtained through root scanner statistical analysis, (b) Scanning images of root systems. Fig. S11. (a) Gene Ontology (GO) enrichment analysis under the inoculation of *S. azotifigens* only (S), *R. deserti* only (R), and co-inoculation of *S. azotifigens* and *R. deserti* (S+R) in the wheat yellow mosaic virus (WYMV) uninfected experimental group. BP: biological processes, CC: cellular components, MF: molecular function. (b) The enrichment analysis of KEGG functional pathways related to plant hormone signal. Fig. S12. (a) Gene Ontology (GO) enrichment analysis under the inoculation of*S. azotifigens* only (S), *R. deserti* only (R), and co-inoculation of *S. azotifigens* and *R. deserti* (S+R) in the wheat yellow mosaic virus (WYMV) infected experimental group. BP: biological processes, CC: cellular components, MF: molecular function. (b) The enrichment analysis of KEGG functional pathways related to plant hormone signal.

Acknowledgements
We thank Zhefei Li from Northwest A&F University for his valuable suggestions.

Authors' contributions
Conceptualization: JC, TG, FW, HL, and HZ. Methodology: FW, HZ, CW, YW, and LZ. Funding acquisition: TG, HZ, JY, and JC. Writing—original draft: FW and HZ. Writing—review and editing: HZ, HL, PC, and TG. All authors reviewed the manuscript.

Funding
This study was financially supported by National Key Research and Development Program (2022YFA1304400, 2022YFD1400700), the "Pioneer" and "Leading Goose" R&D Program of Zhejiang (2023C02016), China Agriculture Research System from the Ministry of Agriculture of P.R. China (CARS-08-G09) and sponsored by the K.C. Wong Magna Fund of Ningbo University.

Data availability
The datasets supporting the conclusions of this article are available in the National Center for Biotechnology Information (NCBI) repository, PRJNA1001824 (https://www.ncbi.nlm.nih.gov/bioproject/PRJNA1001824), and the NCBI Short Read Archive, PRJNA1039684. All data is available for download.

Declarations

Ethics approval and consent to participate
Not applicable.

Consent for publication
Not applicable.

Competing interests
The authors declare no competing interests.

Author details
[1]State Key Laboratory for Managing Biotic and Chemical Threats to the Quality and Safety of Agro-products, Key Laboratory of Biotechnology in Plant Protection of Ministry of Agriculture and Zhejiang Province, Institute of Plant Virology, Ningbo University, Ningbo 315211, China. [2]Hawkesbury Institute for the Environment, Western Sydney University, Penrith, NSW 2753, Australia. [3]National Key Laboratory of Agricultural Microbiology, College of Resources and Environment, Huazhong Agricultural University, Wuhan, China.

Received: 23 January 2024 Accepted: 17 August 2024
Published online: 15 October 2024

References

1. Madden LV, Wheelis M. The threat of plant pathogens as weapons against U.S. crops. Annu Rev Phytopathol. 2003;41(1):155–76.
2. Zhang W. Global pesticide use: profile, trend, cost / benefit and more. Proc Int Acad Ecol Environ Sci. 2018;8:1–27.
3. Arif I, Batool M, Schenk PM. Plant microbiome engineering: expected benefits for improved crop growth and resilience. Trends Biotechnol. 2020;38(12):1385–96.
4. Delgado-Baquerizo M, Reich PB, Trivedi C, Eldridge DJ, Abades S, Alfaro FD, et al. Multiple elements of soil biodiversity drive ecosystem functions across biomes. Nat Ecol Evol. 2020;4(2):210–20.
5. Qiu Z, Egidi E, Liu H, Kaur S, Singh BK. New frontiers in agriculture productivity: optimised microbial inoculants and in situ microbiome engineering. Biotechnol Adv. 2019;37(6):107371.
6. Sun A, Jiao XY, Chen Q, Wu AL, Zheng Y, Lin YX, et al. Microbial communities in crop phyllosphere and root endosphere are more resistant than soil microbiota to fertilization. Soil Biol Biochem. 2021;153(1):108113.
7. Berendsen RL, Vismans G, Yu K, Song Y, de Jonge R, Burgman WP, et al. Disease-induced assemblage of a plant-beneficial bacterial consortium. ISME J. 2018;12(6):1496–507.
8. Santoyo G. How plants recruit their microbiome? New insights into beneficial interactions. J Adv Res. 2022;40:45–58.
9. Goossens PAOX, Spooren J, Baremans KCM, Andel A, Lapin DAO, Echobardo N, et al. Obligate biotroph downy mildew consistently induces near-identical protective microbiomes in *Arabidopsis thaliana*. Nat Microbiol. 2023;8(12):2349–64.
10. Trivedi P, Delgado-Baquerizo M, Trivedi C, Hamonts K, Anderson IC, Singh BK. Keystone microbial taxa regulate the invasion of a fungal pathogen in agro-ecosystems. Soil Biol Biochem. 2017;111:10–4.
11. Bakker P, Berendsen RL, Van Pelt JA, Vismans G, Yu K, Li E, et al. The soil-borne identity and microbiome-assisted agriculture: looking back to the future. Mol Plant. 2020;13(10):1394–401.
12. Chen JP. Occurrence of fungally transmitted *wheat mosaic viruses* in China. Ann Appl Biol. 1993;123:55–61.
13. Guo L, He J, Li J, Chen J, Zhang H. *Chinese wheat mosaic virus:* a long-term threat to wheat in China. J Integr Agric. 2019;18(4):821–9.
14. Chen J. Progress and prospects of studies on *Polymyxa graminis* and its transmitted cereal viruses in China. Prog Nat Sci. 2005;15(6):481–90.
15. Yang J, Zhang T, Li J, Wu N, Wu G, Yang J, et al. *Chinese wheat mosaic virus*-derived vsiRNA-20 can regulate virus infection in wheat through inhibition of vacuolar- (H^+)- PPase induced cell death. New Phytol. 2020;226(1):205–20.
16. Yang S, Liu H, Xie P, Wen T, Shen Q, Yuan J. Emerging pathways for engineering the rhizosphere microbiome for optimal plant health. J Agric Food Chem. 2023;71(11):4441–9.
17. Ohsato S, Miyanishi M, Shirako Y. The optimal temperature for RNA replication in cells infected by *Soil-borne wheat mosaic virus* is 17 ℃. J Gen Virol. 2003;84(4):995–1000.
18. Wu C, Wang F, Ge A, Zhang H, Chen G, Deng Y, et al. Enrichment of microbial taxa after the onset of wheat yellow mosaic disease. Agric Ecosys Environ. 2021;322:107651.
19. Zhang H, Wu C, Wang F, Wang H, Chen G, Cheng Y, et al. Wheat yellow mosaic enhances bacterial deterministic processes in a plant-soil system. Sci Total Environ. 2022;812:151430.
20. Singh BK, Delgado-Baquerizo M, Egidi E, Guirado E, Leach JE, Liu H, et al. Climate change impacts on plant pathogens, food security and paths forward. Nat Rev Microbiol. 2023;21:640–56.
21. Mendes LW, Raaijmakers JM, de Hollander M, Mendes R, Tsai SM. Influence of resistance breeding in common bean on rhizosphere microbiome composition and function. ISME J. 2018;12(1):212–24.
22. Wang X, Wei Z, Yang K, Wang J, Jousset A, Xu Y, et al. Phage combination therapies for bacterial wilt disease in tomato. Nat Biotechnol. 2019;37(12):1513–20.
23. Gu S, Wei Z, Shao Z, Friman VP, Cao K, Yang T, et al. Competition for iron drives phytopathogen control by natural rhizosphere microbiomes. Nat Microbiol. 2020;5(8):1002–10.
24. Akbar A, Han B, Khan AH, Feng C, Ullah A, Khan AS, et al. A transcriptomic study reveals salt stress alleviation in cotton plants upon salt tolerant PGPR inoculation. Environ Exp Bot. 2022;200:104928.
25. Gao Y, Feng J, Wu J, Wang K, Wu S, Liu H, et al. Transcriptome analysis of the growth-promoting effect of volatile organic compounds produced by *Microbacterium aurantiacum* GX14001 on tobacco (*Nicotiana benthamiana*). BMC Plant Biol. 2022;22:208.
26. Bass D, Stentiford GD, Wang HC, Koskella B, Tyler CR. The pathobiome in animal and plant diseases. Trends Ecol Evol. 2019;34(11):996–1008.

27. Qu Q, Zhang Z, Peijnenburg W, Liu W, Lu T, Hu B, et al. Rhizosphere microbiome assembly and its impact on plant growth. J Agric Food Chem. 2020;68(18):5024–38.
28. Mu M, Wang Z, Chen Z, Wu Y, Nie W, Zhao S, et al. Physiological characteristics, rhizosphere soil properties, and root-related microbial communities of Trifolium repens L. in response to Pb toxicity. Sci Total Environ. 2024;907: 167871.
29. Wang F, Wang F, Zhang H, Qin F, Xiang W, Wu C, et al. Deciphering differences in microbial community composition and multifunctionality between healthy and *Alternaria solani*-infected potato rhizosphere soils. Plant Soil. 2022;484(1–2):347–62.
30. Caporaso JG, Kuczynski J, Stombaugh J, Bittinger K, Bushman FD, Costello EK, et al. QIIME allows analysis of high-throughput community sequencing data. Nat Methods. 2010;7(5):335–6.
31. Zhang J, Liu YX, Guo X, Qin Y, Garrido-Oter R, Schulze-Lefert P, et al. High-throughput cultivation and identification of bacteria from the plant root microbiota. Nat Protoc. 2021;16:988–1012.
32. Han Q, Ma Q, Chen Y, Tian B, Xu L, Bai Y, et al. Variation in rhizosphere microbial communities and its association with the symbiotic efficiency of rhizobia in soybean. ISME J. 2020;14:1915–28.
33. van Delden SH, Nazarideljou MJ, Marcelis LFM. Nutrient solutions for *Arabidopsis thaliana*: a study on nutrient solution composition in hydroponics systems. Plant Methods. 2020;16:72.
34. Zhang F, Liu S, Zhang T, Ye Z, Han X, Zhong K, et al. Construction and biological characterization of an infectious full-length cDNA clone of a Chinese isolate of Wheat *yellow mosaic virus*. Virology. 2021;556:101–9.
35. Chen S, Zhou Y, Chen Y, Gu J. fastp: an ultra-fast all-in-one FASTQ preprocessor. Bioinformatics (Oxford, England). 2018;34(17):884–90.
36. Kim D, Langmead B, Salzberg SL. HISAT: a fast spliced aligner with low memory requirements. Nat Methods. 2015;12(4):357–60.
37. Anders S, Pyl PT, Huber W. HTSeq–a Python framework to work with high-throughput sequencing data. Bioinformatics. 2015;31(2):166–9.
38. Roberts A, Trapnell C, Donaghey J, Rinn JL, Pachter L. Improving RNA-Seq expression estimates by correcting for fragment bias. Genome Biol. 2011;12(3): R22.
39. Segata N, Izard J, Waldron L, Gevers D, Miropolsky L, Garrett WS, et al. Metagenomic biomarker discovery and explanation. Genome Biol. 2011;12(6): R60.
40. Meng C, Jiang XS, Wang J, Wei XM, The complex network model for industrial data based on Spearman correlation coefficient. In 2019 International Conference on Internet of Things (iThings) and IEEE Green Computing and Communications (GreenCom) and IEEE Cyber, Physical and Social Computing (CPSCom) and IEEE Smart Data (SmartData). Atlanta, GA, USA; 2019. p. 28–33.
41. Liaw A, Wiener M. Classification and regression by randomForest. R news. 2002;2(3):18–22.
42. Chen G, Wu C, Wang F, Lyu H, Lu Y, Yan C, et al. Microbial community changes in different underground compartments of potato affected yield and quality. 3 Biotech. 2022;12(5):106.
43. Du S, Trivedi P, Wei Z, Feng J, Hu HW, Bi L, et al. The proportion of soilborne fungal pathogens increases with elevated organic carbon in agricultural soils. mSystems. 2022;7(2):e0133721.
44. Love MI, Huber W, Anders S. Moderated estimation of fold change and dispersion for RNA-seq data with DESeq2. Genome Biol. 2014;15(12):550.
45. Albou LP. The gene ontology resource: 20 years and still GOing strong. Nucleic Acids Res. 2019;47(D1):D330–8.
46. Kanehisa M, Araki M, Goto S, Hattori M, Hirakawa M, Itoh M, et al. KEGG for linking genomes to life and the environment. Nucleic Acids Res. 2008;36(Database issue):D480–4.
47. Zhang T, Hu H, Wang Z, Feng T, Yu L, Zhang J, et al. Wheat yellow mosaic virus NIb targets TaVTC2 to elicit broad-spectrum pathogen resistance in wheat. Plant Biotechnol J. 2023;21(5):1073–88.
48. Kwak MJ, Kong HG, Choi K, Kwon SK, Song JY, Lee J, et al. Rhizosphere microbiome structure alters to enable wilt resistance in tomato. Nat Biotechnol. 2018;36(11):1100–9.
49. Singh BK, Trivedi P, Egidi E, Macdonald CA, Delgado-Baquerizo M. Crop microbiome and sustainable agriculture. Nat Rev Microbiol. 2020;18(11):601–2.
50. Raaijmakers JM, Paulitz TC, Steinberg C, Alabouvette C, Moënne-Loccoz Y. The rhizosphere: a playground and battlefield for soilborne pathogens and beneficial microorganisms. Plant Soil. 2008;321:341–61.
51. Luo L, Wang L, Deng L, Mei X, Liu Y, Huang H, et al. Enrichment of *Burkholderia* in the rhizosphere by autotoxic ginsenosides to alleviate negative plant-soil feedback. Microbiol Spectrum. 2021;9(3):e0140021.
52. Ivanova AA, Oshkin IY, Danilova OV, Philippov DA, Ravin NV, Dedysh SN. Rokubacteria in northern peatlands: habitat preferences and diversity patterns. Microorganisms. 2021;10(1): 11.
53. Ding Y, Wei R, Wang L, Yang C, Li H, Wang H. Diversity and dynamics of microbial ecosystem on berry surface during the ripening of ecolly (*Vitis vinifera* L.) grape in Wuhai, China. World J Microbiol Biotechnol. 2021;37(12):214.
54. Asaf S, Numan M, Khan AL, Al-Harrasi A. *Sphingomonas*: from diversity and genomics to functional role in environmental remediation and plant growth. Crit Rev Biotechnol. 2020;40(2):138–52.
55. Khan AL, Waqas M, Kang SM, Al-Harrasi A, Hussain J, Al-Rawahi A, et al. Bacterial endophyte Sphingomonas sp. LK11 produces gibberellins and IAA and promotes tomato plant growth. J Microbiol. 2014;52(8):689–95.
56. Kolp M, Fulbright DW, Jarosz AM. Inhibition of virulent and hypovirulent *Cryphonectria parasitica* growth in dual culture by fungi commonly isolated from chestnut blight cankers. Fungal Biol. 2018;122(10):935–42.
57. Lazar A, Mushinski RM, Bending GD. Landscape scale ecology of *Tetracladium* spp. fungal root endophytes. Environ Microbiome. 2022;17(1):40.
58. Merín MG, Mendoza LM, Morata de Ambrosini VI. Pectinolytic yeasts from viticultural and enological environments: novel finding of Filobasidium capsuligenum producing pectinases. J Basic Microbiol. 2014;54(8):835–42.
59. Urquhart EJ, Punja ZK. Hydrolytic enzymes and antifungal compounds produced by *Tilletiopsis* species, phyllosphere yeasts that are antagonists of powdery mildew fungi. Can J Microbiol. 2002;48(3):219–29.
60. Anzai Y, Kim H, Park JY, Wakabayashi H, Oyaizu H. Phylogenetic affiliation of the pseudomonads based on 16S rRNA sequence. Int J Syst Evol Microbiol. 2000;50 Pt 4:1563–89.
61. Liu Q, Wang S, Li K, Qiao J, Guo Y, Liu Z, et al. Responses of soil bacterial and fungal communities to the long-term monoculture of grapevine. Appl Microbiol Biotechnol. 2021;105(18):7035–50.
62. Zhou X, Wang J, Liu F, Liang J, Zhao P, Tsui CKM, et al. Cross-kingdom synthetic microbiota supports tomato suppression of Fusarium wilt disease. Nat Commun. 2022;13(1):7890.
63. Manamgoda DS, Rossman AY, Castlebury LA, Crous PW, Madrid H, Chukeatirote E, et al. The genus *Bipolaris*. Stud Mycol. 2014;79:221–88.
64. Oliver RP, Friesen TL, Faris JD, Solomon PS. *Stagonospora nodorum*: from pathology to genomics and host resistance. Annu Rev Phytopathol. 2012;50:23–43.
65. Qu P, Aratani A, Syoji T, Toda T, Kubota M, Hyakumachi M. Use of single-protoplast isolates in the study of the mating phenomena of *Rhizoctonia solani* (*Thanatephorus cucumeris*) AG-1 IC and IA. Mycoscience. 2008;49(2):132–7.
66. Gao M, Xiong C, Gao C, Tsui CKM, Wang MM, Zhou X, et al. Disease-induced changes in plant microbiome assembly and functional adaptation. Microbiome. 2021;9(1):187.
67. Lv T, Zhan C, Pan Q, Xu H, Fang H, Wang M, et al. Plant pathogenesis: toward multidimensional understanding of the microbiome. iMeta. 2023;2:e129.
68. Wang S, Zhang X, Zhang Z, Chen Y, Tian Q, Zeng D, et al. *Fusarium*-produced vitamin B6 promotes the evasion of soybean resistance by *Phytophthora sojae*. J Integr Plant Biol. 2023;65:2204–17.
69. Wen T, Xie P, Liu H, Liu T, Zhao M, Yang S, et al. Tapping the rhizosphere metabolites for the prebiotic control of soil-borne bacterial wilt disease. Nat Commun. 2023;14(1):4497.
70. Yin C, Casa Vargas JM, Schlatter DC, Hagerty CH, Hulbert SH, Paulitz TC. Rhizosphere community selection reveals bacteria associated with reduced root disease. Microbiome. 2021;9(1):86.
71. Ratzke C, Barrere J, Gore J. Strength of species interactions determines biodiversity and stability in microbial communities. Nature Ecology & Evolution. 2020;4:376–83.
72. Yin J, Zhang Z, Zhu C, Wang T, Wang R, Ruan L. Heritability of tomato rhizobacteria resistant to *Ralstonia solanacearum*. Microbiome. 2022;10(1):227.
73. Ju W, Liu L, Fang L, Cui Y, Duan C, Wu H. Impact of co-inoculation with plant-growth-promoting rhizobacteria and rhizobium on the biochemical responses of alfalfa-soil system in copper contaminated soil. Ecotoxicol Environ Saf. 2019;167:218–26 Arkhipov A, Carvalhais LC, Schenk PM. PGPR control Phytophthora capsici in tomato through induced systemic resistance, early hypersensitive response and direct antagonism in a cultivar-specific manner. Eur J of Plant Pathol. 2023;167:811–32.

74. Liu H, Li J, Carvalhais LC, Percy CD, Prakash Verma J, Schenk PM, et al. Evidence for the plant recruitment of beneficial microbes to suppress soil-borne pathogens. New Phytol. 2021;229(5):2873–85.
75. Liu X, Matsumoto H, Lv T, Zhan C, Fang H, Pan Q, et al. Phyllosphere microbiome induces host metabolic defence against rice false-smut disease. Nat Microbiol. 2023;8(8):1419–33.
76. Sessitsch A, Hardoim P, Döring J, Weilharter A, Krause A, Woyke T, et al. Functional characteristics of an endophyte community colonizing rice roots as revealed by metagenomic analysis. Mol Plant-Microbe Interact. 2012;25(1):28–36.
77. Verbon EH, Liberman LM. Beneficial microbes affect endogenous mechanisms controlling root development. Trends Plant Sci. 2016;21(3):218–29.
78. Schaller GE, Bishopp A, Kieber JJ. The yin-yang of hormones: cytokinin and auxin interactions in plant development. Plant Cell. 2015;27(1):44–63.
79. Kieber JJ, Schaller GE. Cytokinin signaling in plant development. Development. 2018;145(4):dev149344.
80. Qiu D, Xiao J, Ding X, Xiong M, Cai M, Cao Y, et al. OsWRKY13 mediates rice disease resistance by regulating defense-related genes in salicylate- and jasmonate-dependent signaling. Mol Plant Microbe Interact. 2007;20(5):492–9.
81. He Y, Zhang H, Sun Z, Li J, Hong G, Zhu Q, et al. Jasmonic acid-mediated defense suppresses brassinosteroid-mediated susceptibility to *Rice black streaked dwarf virus* infection in rice. New Phytol. 2017;214(1):388–99.
82. Zhang H, Tan X, Li L, He Y, Hong G, Li J, et al. Suppression of auxin signalling promotes rice susceptibility to *Rice black streaked dwarf virus* infection. Mol plant pathol. 2019;20(8):1093–104.
83. Yang Z, Huang Y, Yang J, Yao S, Zhao K, Wang D, et al. Jasmonate signaling enhances RNA silencing and antiviral defense in rice. Cell Host microbe. 2020;28(1):89–103.
84. Li S, Zhao J, Zhai Y, Yuan Q, Zhang H, Wu X, et al. The *hypersensitive induced reaction 3* (*HIR3*) gene contributes to plant basal resistance via an *EDS1* and salicylic acid-dependent pathway. Plant J. 2019;98(5):783–97.
85. Wang Q, Liu Y, He J, Zheng X, Hu J, Liu Y, et al. *STV11* encodes a sulphotransferase and confers durable resistance to rice stripe virus. Nat Commun. 2014;5(1):476.

Publisher's Note